

## Article

# Phytofabrication of Silver Nanoparticles and Their Potent Antifungal Activity against Phytopathogenic Fungi

Humaira Rizwana <sup>1,\*</sup>, Tethkar Alzahrani <sup>1</sup>, Mona S. Alwahibi <sup>1</sup>, Reem M. Aljowaie <sup>1</sup>,  
Horiah A. Aldehaish <sup>1</sup>, Noura S. Alsaggabi <sup>1</sup> and Rasha Ramadan <sup>2</sup>

<sup>1</sup> Department of Botany and Microbiology, College of Science, King Saud University, Riyadh 11495, Saudi Arabia

<sup>2</sup> Central Laboratory, Female Center for Medical Studies and Scientific Section, King Saud University, Riyadh 11495, Saudi Arabia

\* Correspondence: hrizwana@ksu.edu.sa

**Abstract:** Fungal plant pathogens cause huge losses in agricultural production by decreasing crop yield and quality. To reduce crop loss from fungal damage, various synthetic fungicides are applied indiscriminately in agricultural practice. The majority of synthetic fungicides are non-biodegradable, and several critical human health risks are associated with them. Green synthesis nanotechnology offers an effectual, cost-effective, ecofriendly, and innocuous method for the synthesis of green nanofungicides, an excellent replacement for synthetic chemical fungicides. *Origanum majorana* is an aromatic herb with immense pharmacological and medicinal properties. In this context, the present study used the leaves of *O. majorana* to synthesize silver nanoparticles. The biosynthesized particles showed an absorption peak at 441 nm with ultraviolet-visible spectrophotometry (UV-Vis). The spectra obtained from Fourier transform infrared spectroscopy (FT-IR) of *O. majorana* extract and AgNPs showed a myriad of functional groups corresponding to vital biomolecules that act as capping and reducing agents. The synthesized silver nanoparticles were spheroidal, and their size measured between 8 nm and 42 nm, as depicted by transmission electron microscopy (TEM). The energy-dispersive X-ray spectrum (EDX) showed a silver peak at 3 keV. The phytofabricated silver NPs demonstrated robust inhibitory activity on the mycelial growth of *A. alternata* f sp. *lycopersici* (87%), followed by *Pestalotiopsis mangiferae* (85%), *Macrophomina phaseolina* (78%), and *Colletotrichum musae* (75%). The minimum inhibitory concentration value for *A. alternata* f sp. *lycopersici* and *Pestalotiopsis mangiferae* was 2 µg/mL, while the minimum fungicidal concentrations were 4 and 8 µg/mL, respectively. Additionally, the fabricated AgNPs induced severe damaging and destructive effects to the morphology of hyphae and conidia, as witnessed by scanning electron microscopy studies.



**Citation:** Rizwana, H.; Alzahrani, T.; Alwahibi, M.S.; Aljowaie, R.M.; Aldehaish, H.A.; Alsaggabi, N.S.; Ramadan, R. Phytofabrication of Silver Nanoparticles and Their Potent Antifungal Activity against Phytopathogenic Fungi. *Processes* **2022**, *10*, 2558. <https://doi.org/10.3390/pr10122558>

Academic Editor: Fabio Carniato

Received: 14 November 2022

Accepted: 29 November 2022

Published: 1 December 2022

**Publisher's Note:** MDPI stays neutral with regard to jurisdictional claims in published maps and institutional affiliations.



**Copyright:** © 2022 by the authors. Licensee MDPI, Basel, Switzerland. This article is an open access article distributed under the terms and conditions of the Creative Commons Attribution (CC BY) license (<https://creativecommons.org/licenses/by/4.0/>).

**Keywords:** green synthesis; silver nanoparticles; phytopathogenic fungi; antifungal activity; nanofungicide

## 1. Introduction

Fungal plant pathogens are largely responsible for huge crop losses (70–80%) in the agricultural industry [1,2]. Plants and their produce are highly vulnerable to fungal attack during growth and the postharvest period [3]. Recent upsurges in fungicide-resistant strains of phytopathogenic fungi with a wide host range have further worsened the crisis of plant disease management. Fungal pathogens not only decrease the crop yield but drastically abate its quality [4]. Worldwide chemical fungicide application is an intensively practiced plant disease management strategy. Although chemical fungicides are highly effective, their eco-toxicological and environmental effects cannot be ignored [5]. Hence, the greatest challenge for agro scientists is to develop an alternative eco-friendly disease management strategy to control fungal diseases, boost crop yield, and thus benefit the world economy [6].

Agricultural biotechnology and nanotechnology have emerged as promising tools to indemnify the damages caused to crops by agricultural pests and diseases. Nanotechnology

has gained colossal acceptance through its innovative technology in various fields such as medical sciences, agriculture, pharmaceuticals, and genetics, notably for diagnostic and therapeutic purposes. Modern agricultural practices include revolutionary technological applications and approaches that do not have any hostile effects on living organisms and the surrounding environment, ensuring a safe food supply. Nanoparticles (NPs), nanovectors, nanodevices, and nanoformulations are eventually being employed in agricultural practices to diagnose plant diseases, nutritional deficiencies, plant hormone delivery, the slow and targeted release of agrochemicals, gene transfer, nanobarcoding, nanosized fungicides, pesticides, and fertilizers [7,8].

Recently, inorganic NPs such as iron, silver, carbon, copper, silica, ZnO, and MgO have been successfully used to formulate nanofungicides and nanoemulsions. All the formulated nanohybrids have demonstrated potent inhibitory activity against pathogenic microorganisms [9]. The distinctive properties of NPs, such as their size (1–100 nm), shape, large surface area, and optical and physiochemical properties assist in the formulation of novel fungicides with increased efficacy in controlling fungal plant pathogens [10,11]. In a study, carbon nanomaterial effectively controlled the growth of two phytopathogens, *Fusarium poae* and *F. graminearum* [12].

Silver NPs (AgNPs) stabilized by PVP (polyvinylpyrrolidone) exhibited strong antifungal effects on the growth of *Candida krusei*, *C. albicans*, *C. glabrata*, *C. tropicalis*, and *Aspergillus niger* [13]. In another study, many metal oxide NPs, such as CuO NPs, Fe<sub>2</sub>O<sub>3</sub> NPs, TiO<sub>2</sub> NPs, and carbon nanomaterials, were tested against *Botrytis cinerea* both in vitro and in vivo. CuO NPs and carbon nanomaterials suppressed the mycelial growth and *B. cinerea* infection in a significant manner [14]. Similarly, silver NPs inhibited the colony growth of *Magnaporthe grisea* and *Bipolaris sorokiniana* [15]. However, some researches have unveiled the possible negative effects of chemically synthesized nanoparticles, for instance the use of toxic chemicals, generation of waste, and negative impact on the environment [16,17]. Therefore, there is a need to develop NPs which are biocompatible, sustainable, and harmless to the non-target organisms.

Nanoparticles synthesized using plants and microorganisms are considered as safe nanofactories to manage plant diseases as they are ecofriendly and cost-effective [18,19]. Green synthesis of NPs using plants has several advantages over other methods of synthesis, as they are easier and quicker to synthesize, and the synthesized NPs are stable and free of noxious materials [20]. Green nanosynthesis is an innocuous and reproducible scientific approach as the vast array of phytochemicals in plants function as reducers, stabilizers, redox mediators, and capping agents [21]. Previous studies have demonstrated the antifungal activity of AgNPs synthesized from the fruit peel extracts of pomegranate and orange [22], leaf extracts of *Scoparia dulcis*, *Pouzolzia zeylanica*, and *Phyllanthus urinaria* [23], and flower extracts of *Bauhinia tomentosa* [24]. Silver nanoparticles (AgNPs) have received the most attention among all metal nanoparticles due to their low cost and antimicrobial properties [25]. Hence, in this study, a facile green synthesis of silver nanoparticles was carried out using aqueous leaf extract of *Origanum majorana* in the presence of sunlight.

*Origanum majorana* L. is a perennial aromatic herb and member of the Lamiaceae family. It is native to the Mediterranean region, especially Algeria, Egypt, and Morocco, and is commonly called “sweet marjoram” [26]. In the Kingdom of Saudi Arabia, the herb is locally referred to as doosh, bardaqoosh, or wezzab [27]. The decoction of leaves is used to protect hormone levels in women [28]. *O. majorana* leaves, flowers, and stems are known for their medicinal value, pharmacological effects, and as a seasoning ingredient [29]. In addition, the leaves and flowers are used in folk medicine to treat stomach aches, nervous disorders, congestion, asthma, cough, and indigestion [30–32]. The plant contains polyphenols, phenolic glycosides, proteins, amino acids, vitamin C, triterpenoids, and tannins [29,33,34]. Previous studies have demonstrated potent anticancer, anti-inflammatory, nephrotoxicity protective, antipyretic, and analgesic effects of *O. majorana* [35,36]. *O. majorana* leaves were chosen for this study because of their medicinal and pharmacological properties.

## 2. Materials and Methods

### 2.1. Instruments, Chemical and Culture Media

An ultraviolet-visible spectrophotometer (Shimadzu, Kyoto, Japan; model No. 1800) was used to capture SPR peaks of nanoparticles. A transmission electron microscope (TEM-JEOL JEM-Plus-1400, Tokyo, Japan) was used to measure the size and shape of synthesized nanoparticles. A Fourier transform infrared spectroscope (FTIR-Thermo Scientific, Waltham, MA, USA, Model-Nicolet-6700) was used to identify the functional groups of the synthesized AgNPs and extract. A scanning electron microscope (SEM; JEOL-Model JSM-6060LV, Japan) was used to examine fungal isolates treated with AgNPs. The chemicals (silver nitrate-AgNO<sub>3</sub>, ethanol, and fungicide) and fungal culture media (potato dextrose agar-PDA) were bought from Sigma-Aldrich (Saint Louis, MI, USA). For various experiments, ultra-pure water and distilled water were used.

### 2.2. Aqueous Leaf Extract Preparation

Fresh *O. majorana* was purchased from a local market in Medina Al Munawarah, Saudi Arabia. The leaves were carefully detached from the stem and washed thoroughly. To 100 mL of distilled water, roughly chopped *O. majorana* leaves were added, and the mixture boiled for about 20 min. After the mixture cooled, it was filtered using Whatman's filter paper, No. 1, and the filtrate was centrifuged at 5000 × g rpm. The filtered aqueous extract was used for the experimental work conducted in the present study.

### 2.3. Plant Pathogenic Fungi

The fungal phytopathogens, *Colletotrichum musae*, *Alternaria alternata*, *Macrophomina phaseolina*, *Pestalotiopsis mangiferae*, *Fusarium oxysporum*, and *Botrytis cinerea*, were provided by the Department of Plant Protection, College of Food and Agricultural Sciences, King Saud University, Riyadh, Saudi Arabia.

### 2.4. Nanosynthesis from Leaves of *O. majorana*

A 1 mM aqueous silver nitrate solution (AgNO<sub>3</sub>) was prepared by adding a fixed amount of silver nitrate powder to 100 mL of distilled water. To 45 mL of aqueous silver nitrate solution (AgNO<sub>3</sub>), 5 mL of aqueous *O. majorana* leaf extract was added, and this mixture was exposed to direct sunlight. The time required to change its original color was monitored and recorded.

### 2.5. Characterization of the Synthesized AgNPs by UV-Vis, TEM, EDX and DLS

Upon exposure to direct sunlight, the mixture of silver nitrate (AgNO<sub>3</sub>) and *O. majorana* extract changed its original color to brown, signaling the formation of ORM-AgNPs. A UV-Vis spectroscopic analysis was conducted to authenticate the nanosynthesis, and the absorption peak was obtained on an ultraviolet-visible spectrophotometer (Shimadzu, Japan—model No. 1800). The characterization of *O. majorana*-AgNPs included determining the size and shape of biosynthesized silver NPs using a transmission electron microscope (TEM-JEOL JEM-Plus-1400, Tokyo, Japan). Particle size distribution was obtained by measuring 200 particles using image version 1.8.0, and a histogram was plotted with origenPro 2023. The dynamic light scattering analyzer (DLS) measured the size distribution in suspension and the polydispersity index (PDI on a Zeta sizer (ZS), model-Nano Series-ZEN-3600, Malvern, UK). The field emission scanning electron microscope coupled with an energy dispersive X-ray detector (FESEM-EDAX-JSM-7610F-Japan) captured the elemental composition of the biosynthesized AgNPs at 30 kV. An infrared (IR) spectrum of *O. majorana* extract and biosynthesized silver NPs was obtained with a Fourier transform infrared spectroscope (FTIR-Thermo Scientific, USA, Model-Nicolet-6700). The samples were scanned in the range of 4000–400 cm<sup>-1</sup> with a KBr pellet.

### 2.6. Effect of Biosynthesized AgNPs on the Colony Growth of Phytopathogenic Fungi

Pure fungal cultures of *Colletotrichum musae*, *Alternaria alternata*, *Macrophomina phaseolina*, *Pestalotiopsis mangiferae*, *Fusarium oxysporum*, and *Botrytis cinerea* were sub-cultured on potato dextrose agar (PDA) for 7 days prior to the antifungal assay. The inhibitory effect (in vitro) of synthesized AgNPs on the growth of different fungal isolates was assessed with the method of Kim et al., 2012 [37]. Precisely, 500 µL of synthesized AgNPs, was added to molten PDA agar in separate test tubes and mixed well. The amended PDA media was transferred to sterile Petri dishes and left at 25 °C to solidify. A 6 mm disc was removed from the periphery of each sub-cultured fungal colony and placed (upside down) in the center of the amended PDA plate. Positive and negative controls were PDA amended with the fungicide carbendazim (1%) and plates containing only the PDA media and fungal mycelial disc. All the treated PDA plates, including the control plates, were incubated (28 °C for 7 days). The treatments were run in triplicate, and all the fungal test isolates were tested following the aforesaid method. On the seventh day, the growth of the colony was observed for all the treatments and compared with the control. The colony diameter of treated fungal isolates and control (not treated) was measured (mm), and the percent (%) growth inhibition of each isolate was assessed.

### 2.7. Minimum Inhibitory Concentration (MIC) and Minimum Fungicidal Concentration (MFC)

The minimum inhibitory concentration (MIC) of the synthesized *O. majorana*-AgNPs against fungal test isolates was determined by the broth dilution method with slight modifications [38]. A series of two-fold serial dilutions of the synthesized AgNPs and fungicide were made separately, and the concentrations ranged from 0.5 to 128 µg/mL. For the MIC assay, potato dextrose broth was used. Equal volumes of broth, spore suspension of test fungal isolates ( $2 \times 10^6$  CFU/mL), and AgNPs were mixed well and placed in an incubator at 28 °C for 72 h. All the concentrations were tested in triplicate. Spore suspension and PDA broth without AgNPs served as negative controls, while broth, spore suspension of test fungal isolates ( $2 \times 10^6$  CFU/mL), and the fungicide were regarded as positive controls. The treated suspensions were placed in an incubator at 28 °C for 7 days and observed every 24 h until 72 h, after which the readings were recorded. The lowest concentration that did not show any visible growth in the tubes was regarded as the MIC. The MFC was determined by removing 100 µL of the mixture from tubes exhibiting the MIC concentration and transferring it to potato dextrose agar plates. The plates were incubated for 72 h at 28 °C. The concentrations that did not grow on PDA agar medium were designated as their MFC [39].

### 2.8. Morphology of Treated and Untreated Fungal Isolates as Observed under a Scanning Electron Microscope (SEM)

The morphological alterations in the treated fungi at their MIC concentrations were microphotographed with a scanning electron microscope. For comparative purposes, negative control samples were also subjected to SEM. A fixed amount of fungal suspensions at their MIC concentrations was centrifuged at 8000 rpm for 5 min, then transferred into a sterile tube containing glutaraldehyde (2.5%). Further, after 2 days, this suspension was centrifuged, rinsed three times with tris-acetate buffer (0.1 mol/L, pH 7.2), and then subjected to dehydration with ethanol in a series of concentrations (60–100%). After dehydration, the samples were freeze-dried (critical point dryer) and then mounted on stubs coated with gold. Finally, microphotographs were captured on an SEM model (JSM-6060LV-JEOL) from Japan Ltd.

### 2.9. Statistical Analysis

The data presented in tables and figures in this study represented values from experiments run in triplicate ( $\pm$ SD). Graph Pad Prism (8.4.3.686), along with XLSTAT (2020), was used to evaluate the significant differences ( $p \leq 0.05$ ), and Tukey's HSD tests and analysis of variance ANOVA ( $p \leq 0.05$ ) were performed.

### 3. Results and Discussion

#### 3.1. Characterization of Synthesized of ORM-AgNPs

Synthesis of nanoparticles under direct sunlight is a quick, facile, and efficient method of nanosynthesis. In this study, sunlight-irradiated green synthesis was successfully achieved using aqueous leaf extracts of *Origanum majorana*. Leaf extract of *O. majorana* was added to aqueous silver nitrate, and the glass beaker containing the concoction was exposed to direct sunlight to initiate the process of nanosynthesis. Within a few seconds of exposure to direct sunlight, the concoction slowly changed color. After 5 min, the original color (dark buff) of the concoction changed to a deep brown (Figure 1). The color change signified the completion of the nucleation and subsequent reduction (silver ions to silver NPs). The formation of *O. majorana*-AgNPs was inferred by the brown color of the reaction mixture. The UV-Vis spectroscopic analysis of the brown reaction mixture displayed a distinctive peak at 441 nm on the absorption spectrum. This peak corroborates the presence of AgNPs and is related to surface plasmon resonance (Figure 2). Comparable to the findings of this study, another study on *O. majorana*-AgNPs demonstrated an absorption peak at 440 nm [40]. The excitation of electrons resulting from plasmon resonance with characteristic optoelectronic properties, particularly in metal Nps, results in UV-Vis absorption peaks in the range between 410–550 nm [41–43]. Previous reports have also shown rapid synthesis of AgNPs under direct sunlight from extracts of *Citrus limon* and *Andrachnea chordifolia* [44,45]. The phytochemicals present in the *O. majorana* extract could have assisted in the reduction of  $\text{Ag}^+$  to  $\text{Ag}^0$ . Light-induced reduction has gained popularity in nanosynthesis as the reduction of metal ions can be carried out in a controlled manner with small amounts of reducing agents; it does not require any special light-absorbing agents; and the photo-induced methods are cost effective, eco-friendly, and competitive [46]. Most importantly, the process is very rapid compared to dark conditions [45]. Most importantly, the process is very rapid compared to the dark conditions [45]. The sunlight acts like a catalyst and induces the process of kinetic reaction of silver salts with the functional groups of secondary metabolites present in plant extract, enabling nanosynthesis in a few minutes in comparison to dark conditions, which take a longer duration [47,48]. The formation of AgNPs within 5 min in the current study amply demonstrated that the sunlight acted as a photocatalyst during the reduction processes; therefore, the green silver nanosynthesis facilitated by sunlight is a sustainable, quick, non-hazardous, and economical process.

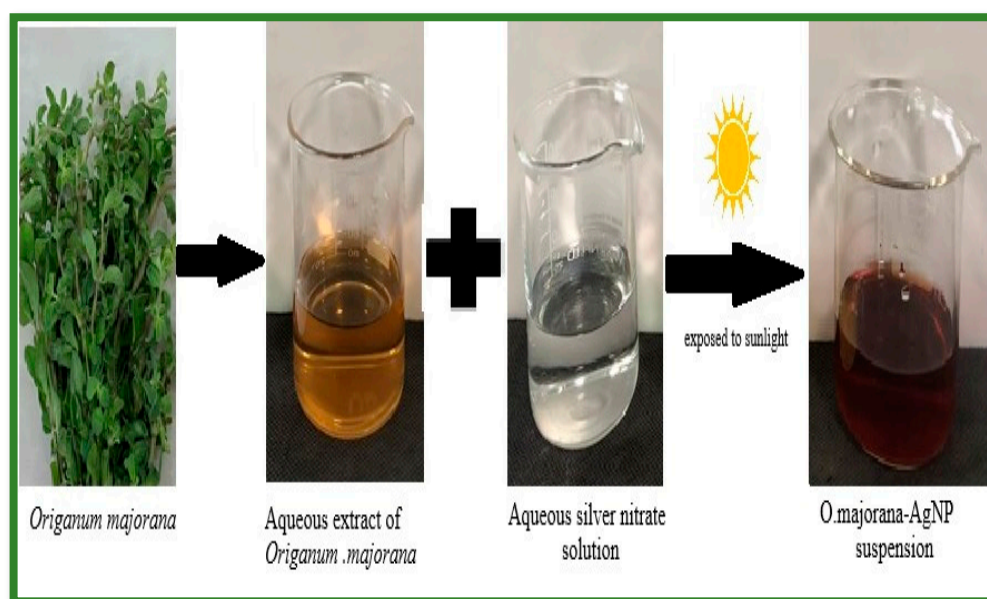


**Figure 1.** Phytofabrication of silver NPs from aqueous leaf extracts of *Origanum majorana*.

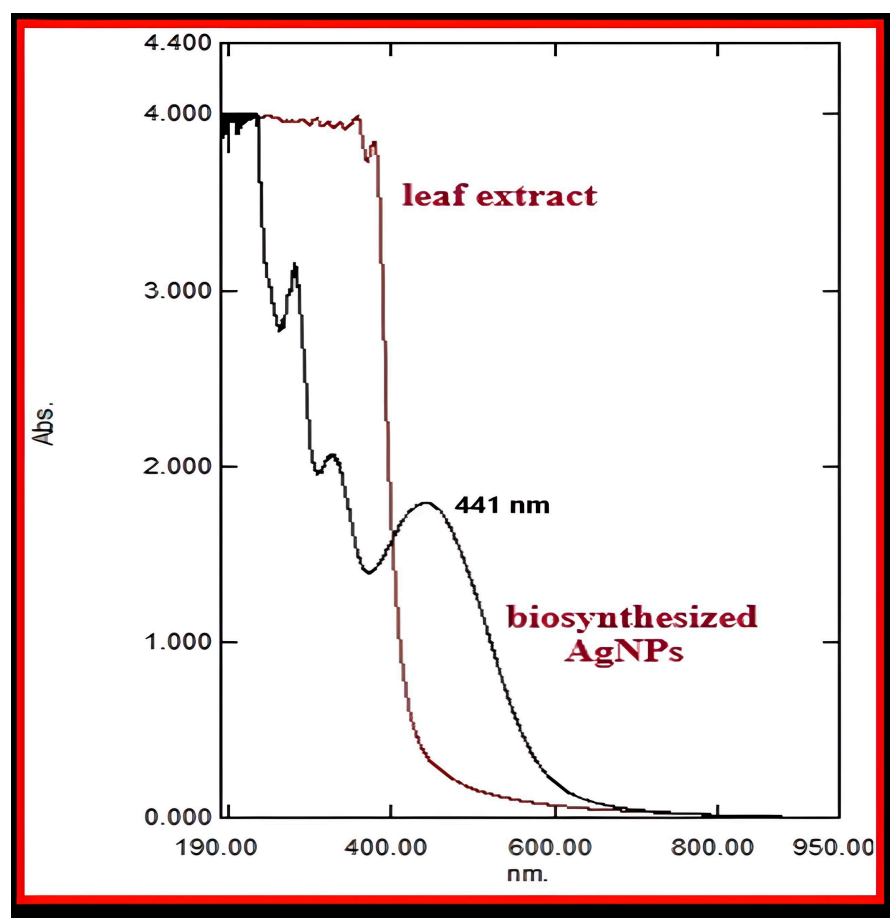


**Figure 2.** Absorption spectra of silver NPs synthesized using *O. majorana* aqueous leaf extract.

### 3.2. Fourier Transform Infrared Spectroscopy (FTIR) Analysis of Aqueous Extract of *O. majorana* and Synthesized AgNPs

*O. majorana* aqueous extract and synthesized AgNPs were studied by Fourier transform infrared spectrometry. FTIR gives an insight into the different functional groups present in the extracts and AgNPs. The bioactive functional groups present in plant extracts aid in capping and bio reduction during green nanosynthesis. Hence, analysis of both the extract and synthesized nanoparticles helps us understand the role of the functional groups during nanosynthesis. Figure 3 depicts the FTIR spectra of the extract and biogenic AgNPs. The FTIR spectrum of the aqueous extract showed peaks at  $3752\text{ cm}^{-1}$  and  $3375\text{ cm}^{-1}$ , while the spectrum of biosynthesized AgNPs showed stretching vibrational peaks at  $3753\text{ cm}^{-1}$ ,  $3549\text{ cm}^{-1}$ ,  $3473\text{ cm}^{-1}$ , and  $3416\text{ cm}^{-1}$ . All of the aforementioned peaks arose from O–H stretches of alcohols and phenols as well as N–H stretches of amines. Several other peaks that were observed in the FTIR spectrum of *O. majorana* leaf extract and AgNPs are as follows: Peaks at  $2926\text{ cm}^{-1}$  and  $2369\text{ cm}^{-1}$  corresponded to C–H symmetric and asymmetric stretching vibrations of alkanes, and peaks between  $1511\text{ cm}^{-1}$  and  $1620\text{ cm}^{-1}$  corresponded to C=C stretching of -unsaturated ketone and aromatic rings, poly phenol carbonyl groups (C=O), and N–H bending vibrations of carbonyl amide (I) and N–O stretching. A medium peak at  $1406\text{ cm}^{-1}$  observed in the IR spectrum of *O. majorana* leaf extract denoted the O–H bending of alcohols. The O–H stretching vibrations of alcohols or phenols were witnessed at  $1304\text{ cm}^{-1}$  in the spectrum of silver NPs. Bands detected at  $1262\text{ cm}^{-1}$ ,  $1217\text{ cm}^{-1}$ , and  $1215\text{ cm}^{-1}$  on both the spectra (aqueous extract and silver NPs) arose from the vibrations caused by esters (C–O) and amines (C–N) and aromatic amines. In addition, the peaks at  $1072\text{ cm}^{-1}$ ,  $1074\text{ cm}^{-1}$ ,  $891\text{ cm}^{-1}$ , and  $831\text{ cm}^{-1}$  corresponded to the C–O stretching of alcohols and the bending of alkenes (C=C).

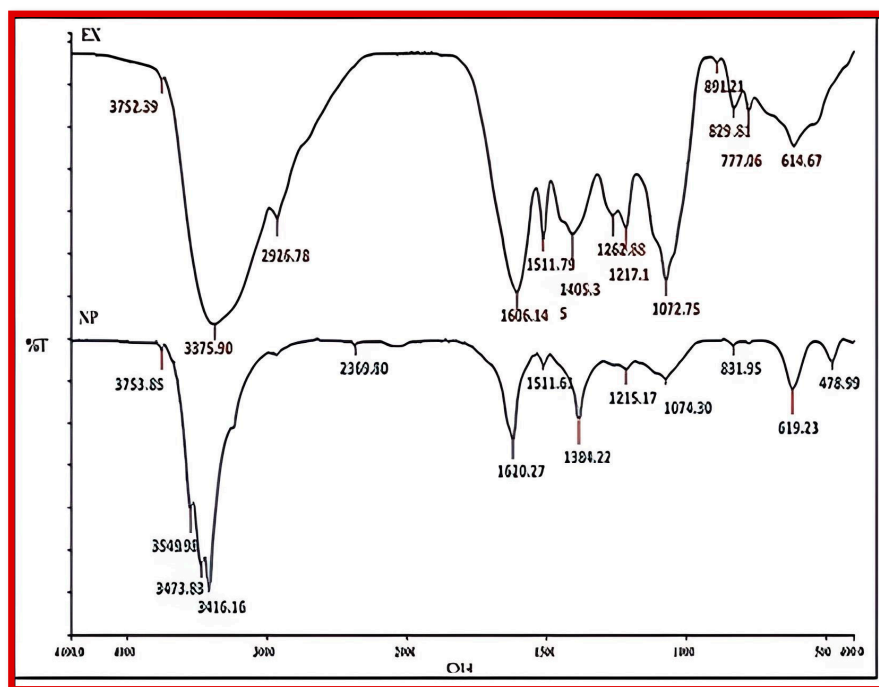


**Figure 3.** Infrared spectra of leaf extract of *O. majorana* and synthesized silver nanoparticles. The FTIR spectra were captured at 4000–400/ $\text{cm}^{-1}$  (Thermo Fischer Nicolet Spectrometer). FTIR spectrum depicts several peaks that correspond to some important functional groups of secondary metabolites present in the samples (Ex—extract; NP—synthesized AgNPs).

A comparative analysis of the IR spectra of extracts with those of synthesized AgNPs showed variations in peak positions. The IR spectrum of *O. majorana*-AgNPs showed some new peaks at 3754  $\text{cm}^{-1}$ , 3473  $\text{cm}^{-1}$ , 3416  $\text{cm}^{-1}$ , 2369  $\text{cm}^{-1}$ , and 1384  $\text{cm}^{-1}$ . Furthermore, the bands of *O. majorana* extract at 2926  $\text{cm}^{-1}$ , 1405  $\text{cm}^{-1}$ , and 777  $\text{cm}^{-1}$  were shifted to 2369  $\text{cm}^{-1}$ , 1384  $\text{cm}^{-1}$ , and 619  $\text{cm}^{-1}$ , respectively, in the spectrum of biosynthesized AgNPs. The shifts of vibrational bands to lower frequencies in the synthesized silver NPs spectrum insinuate the role of phenols, flavonoids, carbonyl groups, and amine groups present in *O. majorana* extracts in nanosynthesis, i.e., reduction (metal salt to ions) and in the capping process [40,49–51]. A thin layer observed around the synthesized AgNPs further corroborates the role of biomolecules in stable capping. In accordance with the present findings, the FTIR spectrum of aqueous leaf extract, biosynthesized AgNPs, cerium oxide NPs, and zinc oxide NPs showed peaks that corresponded to alcohols, phenols, flavonoids, amino acids, proteins, carbonyl groups, ketones, and aldehydes [52–54]. The biomolecules present in plant extracts, such as hydroxyl groups of phenols, carbonyl groups of proteins, and amines, prevent aggregation and are vital in stabilizing the NPs during the bio reduction and capping processes [55]. According to the findings of the FTIR spectrum in this study, hydroxyl groups (OH), carboxyl groups (C-OH), aromatic compounds (C=C), and amines (N-H) could have contributed to the capping and reduction process.

### 3.3. Transmission Electron Microscopy and Dynamic Light Scattering Studies

Figure 4 displays the variable dimension of the photosynthesized silver NPs, which ranged between 2 nm and 42 nm, with an average size of 16.84 nm. The synthesized silver nanoparticles were roughly spheroidal and quasi spherical. The TEM microphotographs of biosynthesized AgNPs showed that the NPs were well dispersed. The hydrodynamic diameter and polydispersity index (PDI) of the NPs were analyzed by the zeta sizer, and the DLS spectrum is depicted in Figure 5. The Z-average size of the *O. majorana*-AgNPs was 74.77 nm, while the PDI was 0.309. The trivial discrepancy in the size of NPs observed in DLS and TEM points to the fact that DLS measures the NPs in a hydrated state, and the

measurements are inclusive of the size of biomolecules and the ions adhering to the surface, creating an adsorbed layer that surrounds AgNPs. Conversely, the TEM measurements are obtained in a dry state [56,57]. Additionally, the weak dispersion and the agglomeration of nanoparticles in an aqueous state considerably increase the average size of the particles, thereby contradicting the measurements of TEM [58]. Validating the present findings, a recent study reported spherical and small-sized (25–50 nm) AgNPs synthesized from aqueous extracts of *O. majorana* [40]. Yet another study showed feather-like *O. majorana*-AgNPs, and their size ranged between 40 and 70 nm [59]. The small, polydispersed nanoparticles reported in this study indicate their potency in inhibiting the growth of fungi.

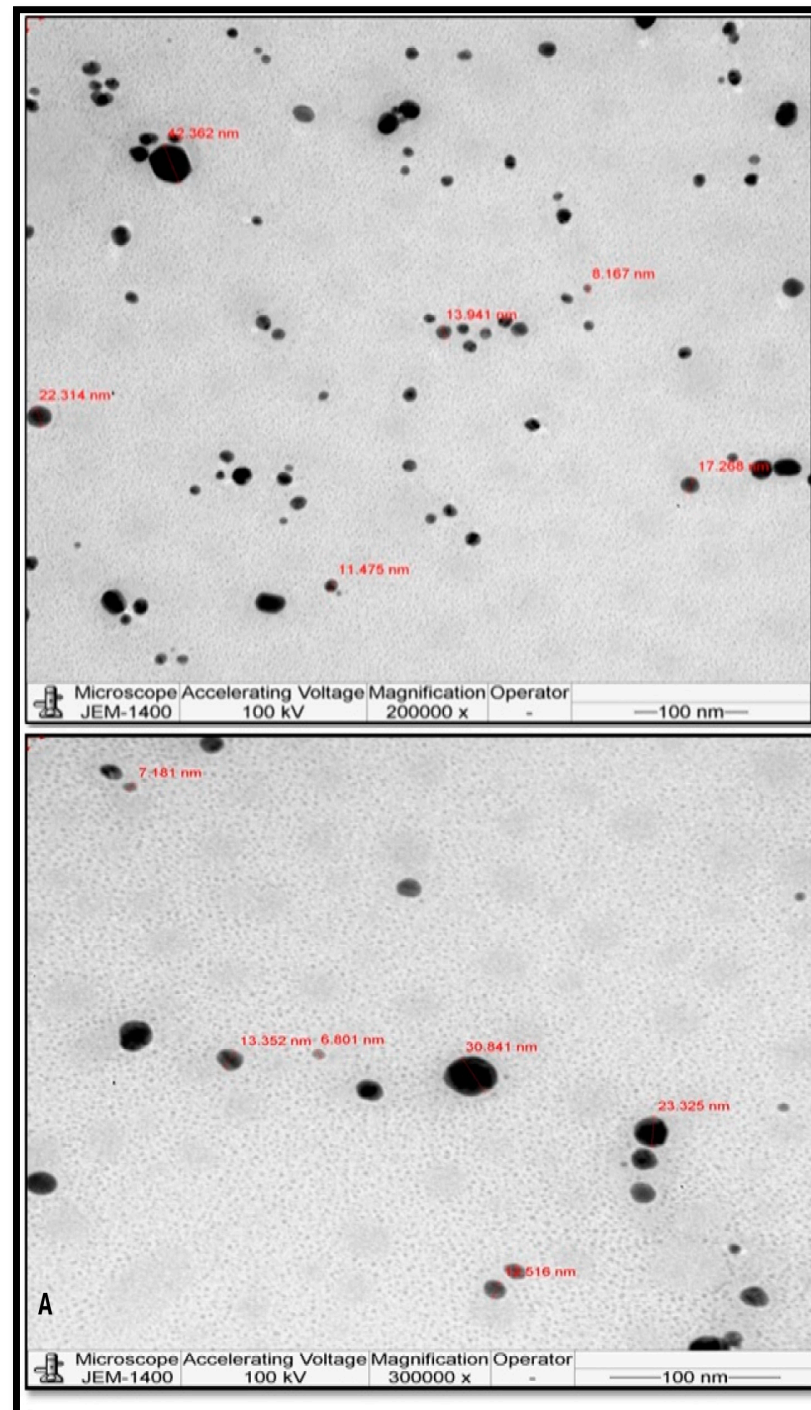
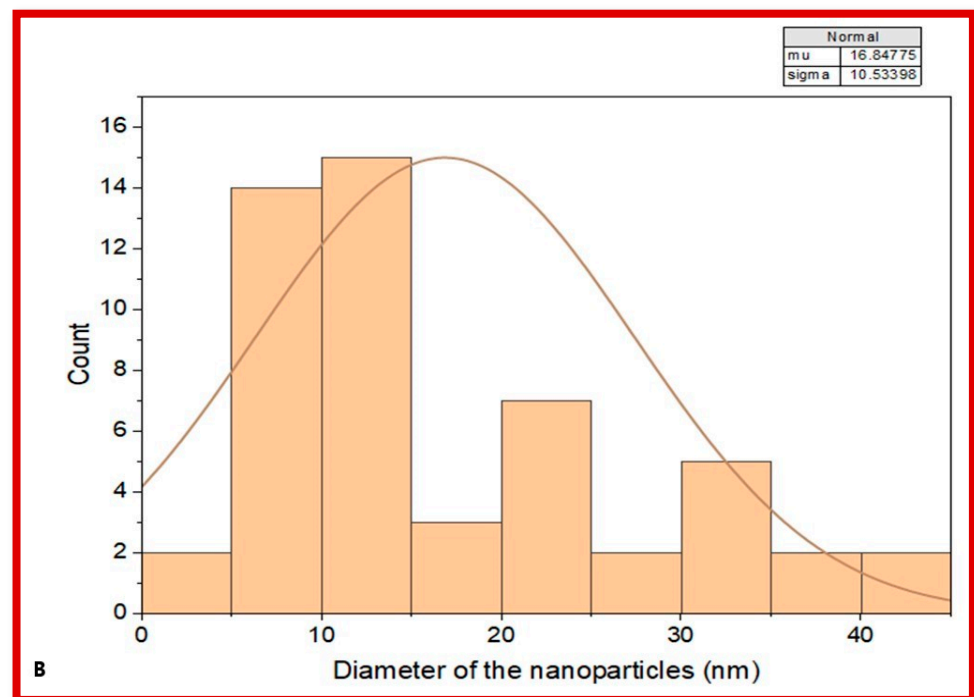
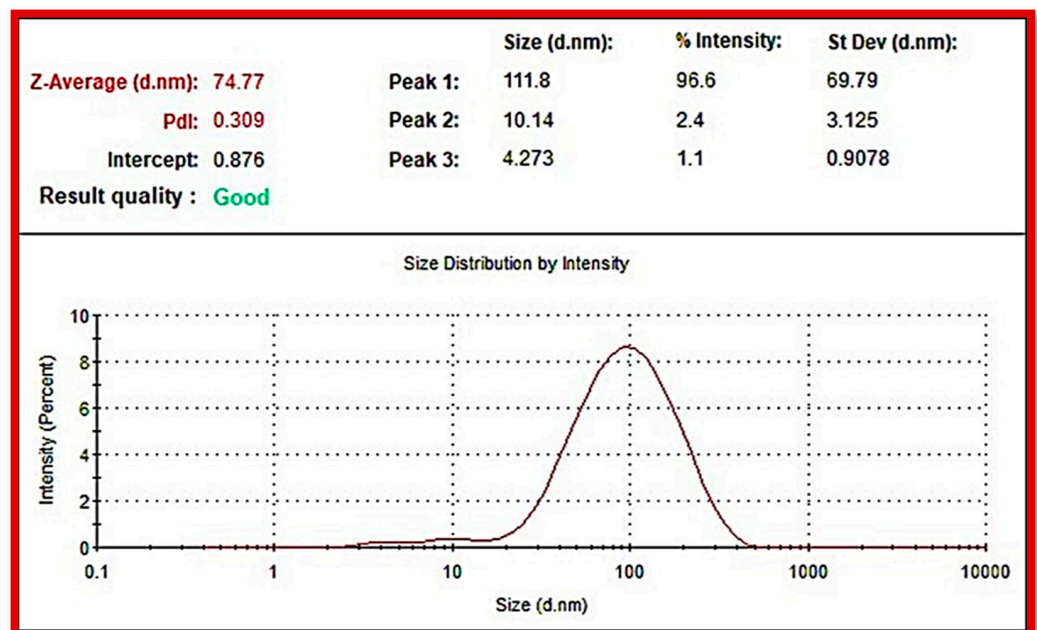


Figure 4. Cont.



**Figure 4.** (A). Transmission electron microphotograph depicting the size and shape of the biosynthesized AgNPs. 4 (B). Histogram of the diameter and the size distribution of the of the silver nanoparticles.



**Figure 5.** The Z-average diameter of the biosynthesized AgNPs and the polydispersity index (PDI) as depicted in the dynamic light scattering (DLS) spectrum.

### 3.4. Elemental Composition of Biosynthesized AgNPs (FESEM-EDX)

The elemental composition of the synthesized AgNPs was confirmed with a field emission scanning electron microscope coupled with an energy dispersive X-ray spectroscopy. The EDX spectrum of *O. majorana*-NPs is shown in Figure 6. The spectrum clearly portrays a signal at 3 keV, substantiating the existence of silver, which is attributable to SPR. Several signals arising from different elements such as iron, chlorine, zinc, potassium, aluminum, and sodium were also witnessed on the spectrum. All the aforementioned elements except

silver could be constituents of the leaf extract of *Origanum majorana* that serve as capping ligands during the synthesis of nanoparticles. In comparison to this study, previous studies depicted the presence of K, Cl, and Al in the EDX spectrum of biosynthesized AgNPs [60,61]. Furthermore, elements such as potassium, aluminum, chlorine, and zinc have been reported in the EDX spectra of plants such as *Trigonella foenum-graecum* [61] and *Sisymbrium irio* [62]. Most importantly, all these elements are considered to be fundamental capping agents [62,63]. Based on the EDX spectrum, the silver peak and signals from other elements indicate successful nucleation by biomolecules present in *O. majorana*.

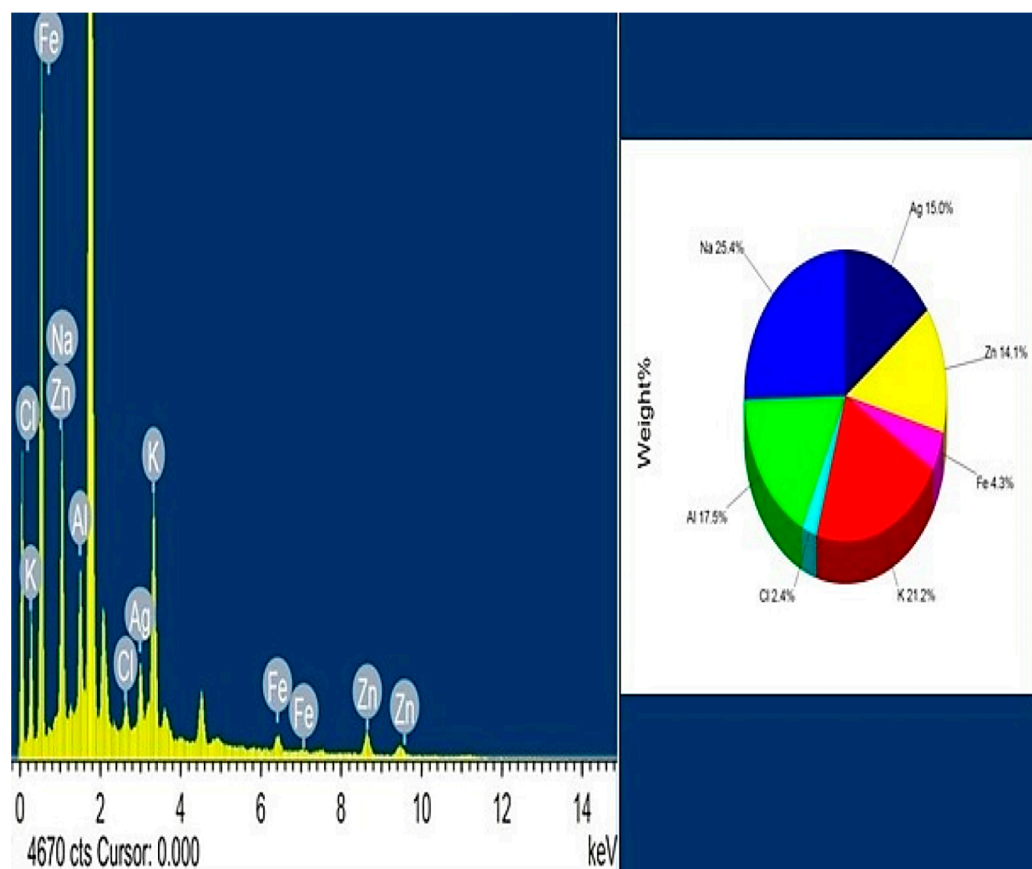


**Figure 6.** Energy dispersive X-ray spectrum (EDX) of the biosynthesized AgNPs. The spectrum shows silver absorption peak at 3 keV.

### 3.5. Mycelial Growth Inhibition of Phytopathogenic Fungi

Phytopathogenic fungi cause enormous crop loss due to plant diseases. Figures 7 and 8 illustrates the robust mycelial growth inhibition of phytopathogenic fungal test isolates by the synthesized silver NPs. (Figure 7A–F). The figure clearly displays that the synthesized NPs significantly arrested the mycelial growth, and in some cases the inhibitory activity was equivalent to the antifungal activity of the fungicide (1% carbendazim). However, *O. majorana* aqueous extracts and silver nitrate solution did not cause substantial growth inhibitory activity on all the test isolates. The *O. majorana* -AgNPs exhibited highest mycelium growth inhibition of *A. alternata* f sp. *lycopersici* (87%), followed by *Pestalotiopsis mangiferae* (85%), *Macrophomina phaseolina* (78%) and *Colletotrichum musae* (75%). However, *B. cinerea* showed poor inhibition of mycelial growth (8%), while *Fusarium oxysporum* did not show inhibitory activity, indicating the ineffectiveness of synthesized AgNPs in controlling the mycelial growth (Figures 8 and 9). The fungicide (positive control) showed strong inhibitory activity against all the tested fungal isolates. It was also observed that the inhibitory effects of the fungicide on *P. mangiferae* (86%) and *A. alternata* f sp. *lycopersici* (85%) were in close proximity to the inhibition caused by biosynthesized AgNPs. Hence, based

on the antifungal growth profiles, AgNPs were quite sturdy in controlling and inhibiting the growth of test fungi. Similar to the present study, purified compounds from leaf extracts of *O. majorana* conjugated with gold nanoparticles (AuNps) inhibited *Aspergillus niger* (73%) and *Candida albicans* (65%) more competently than the component alone [64]. *Rhizoctonia oryzae-sativae*, *Aspergillus parasiticus*, *Altemaria brassicicola*, *Fusarium solani*, *A. niger*, *Candida albicans*, and *Rhizopus oryzae* showed strong inhibition with methanol extracts of *O. majorana* [31]. Previous reports have shown robust antibiofilm and antifungal activity of essential oils of *O. majorana* against *Candida albicans*, *C. tropicalis*, *C. krusei*, *C. dubliniensis*, *Botrytis cinerea*, *Monilinia fructicola*, *Penicillium expansum*, and species of *Aspergillus* [29,65,66]. Similarly, AgNPs derived from leaves of other small herbs have demonstrated significant antifungal activity in prior studies [62,67].

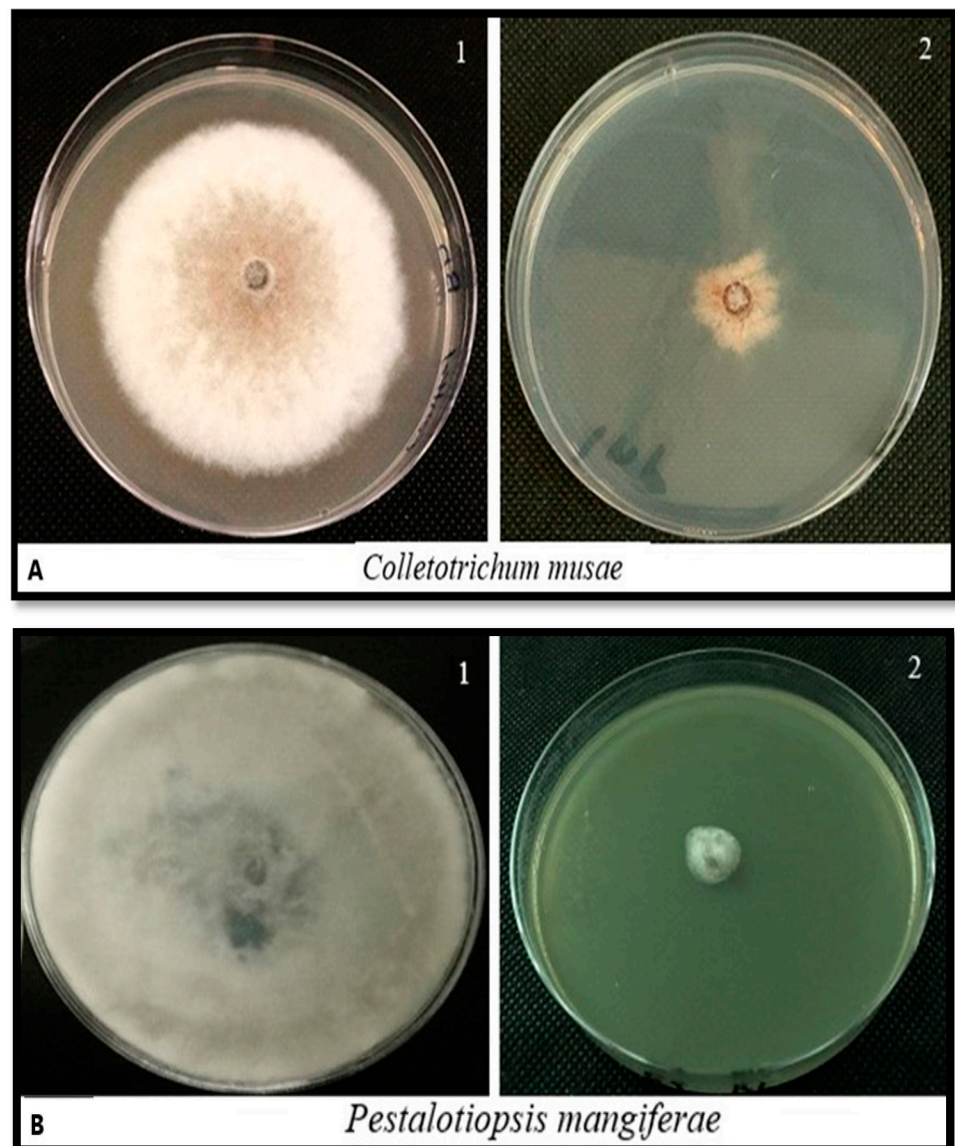


Figure 7. Cont.

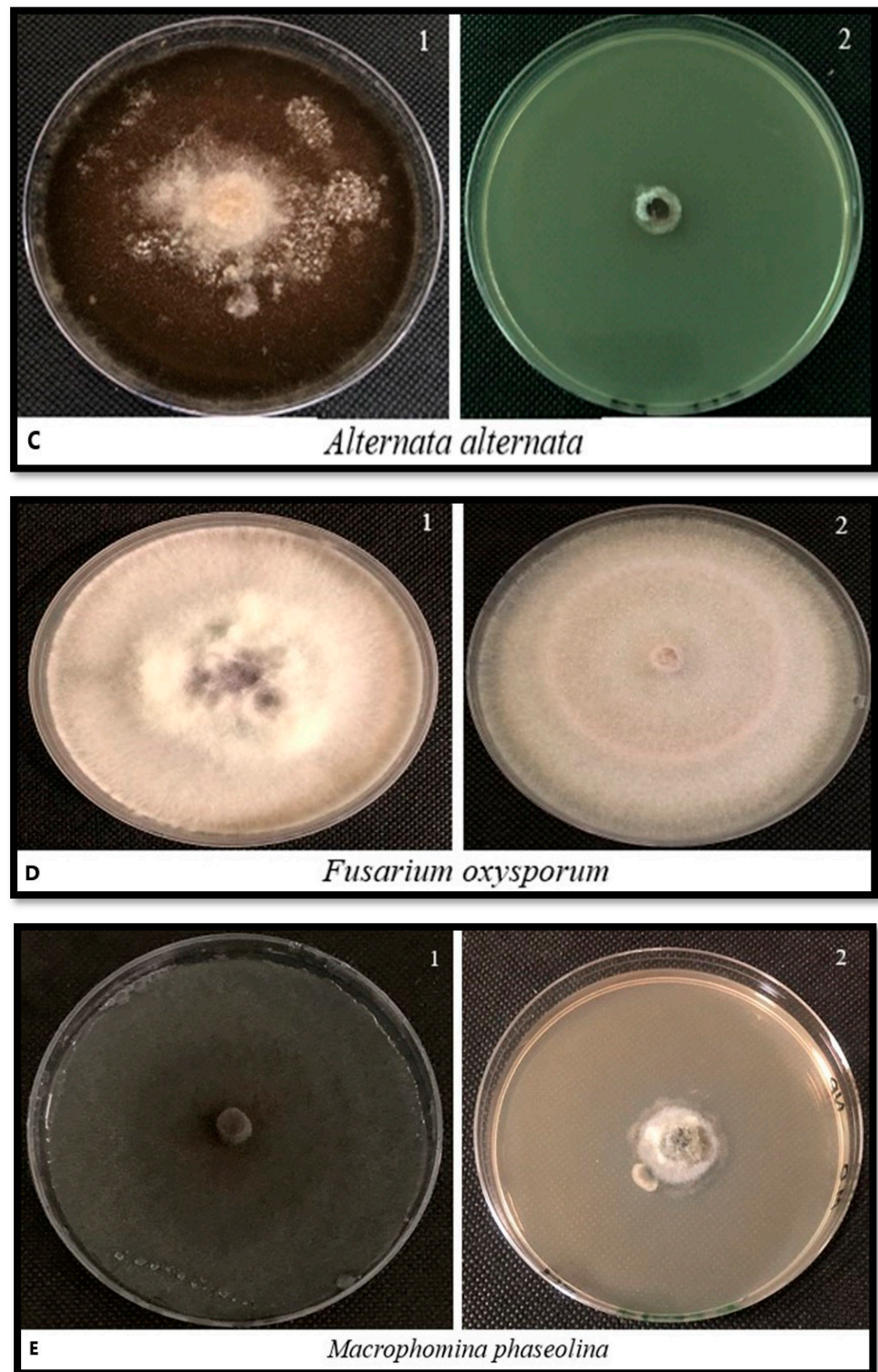
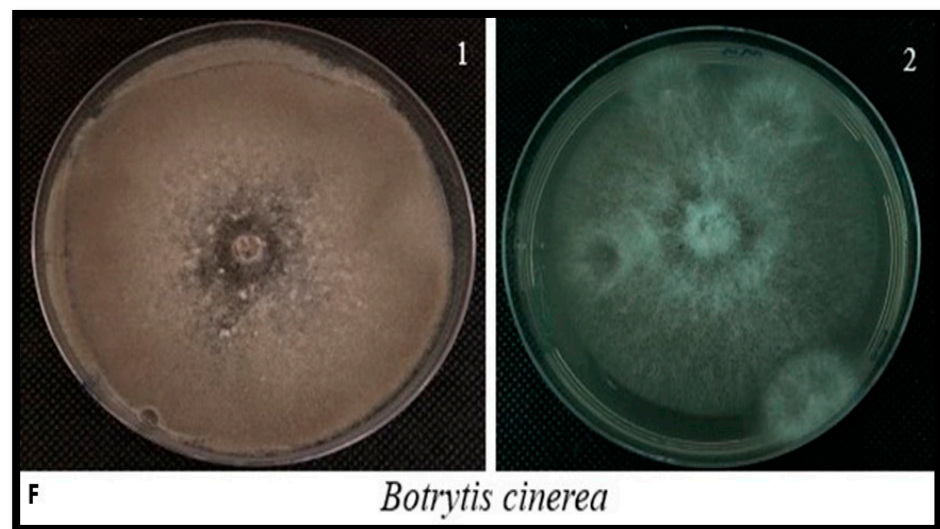
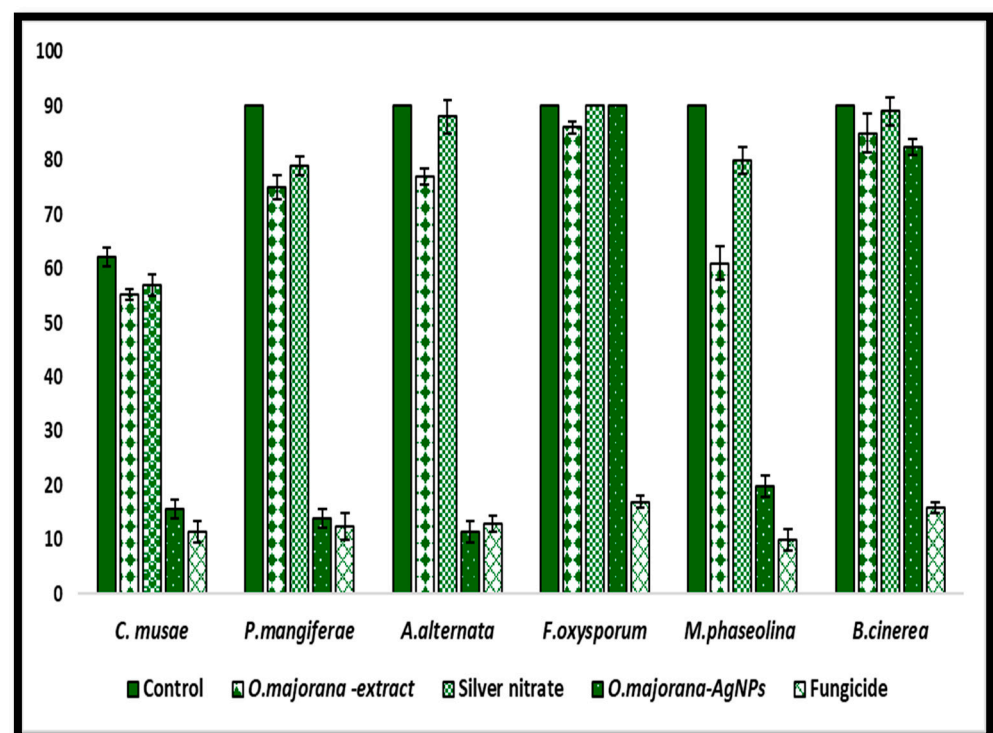


Figure 7. Cont.



**Figure 7.** Effect of the biosynthesized silver nanoparticles on the colony growth of fungal test isolates (A–F). (A) *Colletotrichum musae*; (B) *Pestalotiopsis mangiferae*; (C) *Alternaria alternata*; (D) *Fusarium oxysporum*; (E) *Macrophomina phaseolina*; (F) *Botrytis cinerea*. 1—control (not treated); 2—treated with *O. majorana*-AgNPs.



**Figure 8.** Antifungal activity of fungal isolates treated with *O. majorana*-AgNPs, extracts, silver nitrate, and carbendazim-1%. The graph shows diameter of fungal colony (mm). The values exhibited in the figure are means of three replicates ( $\pm$ SD).

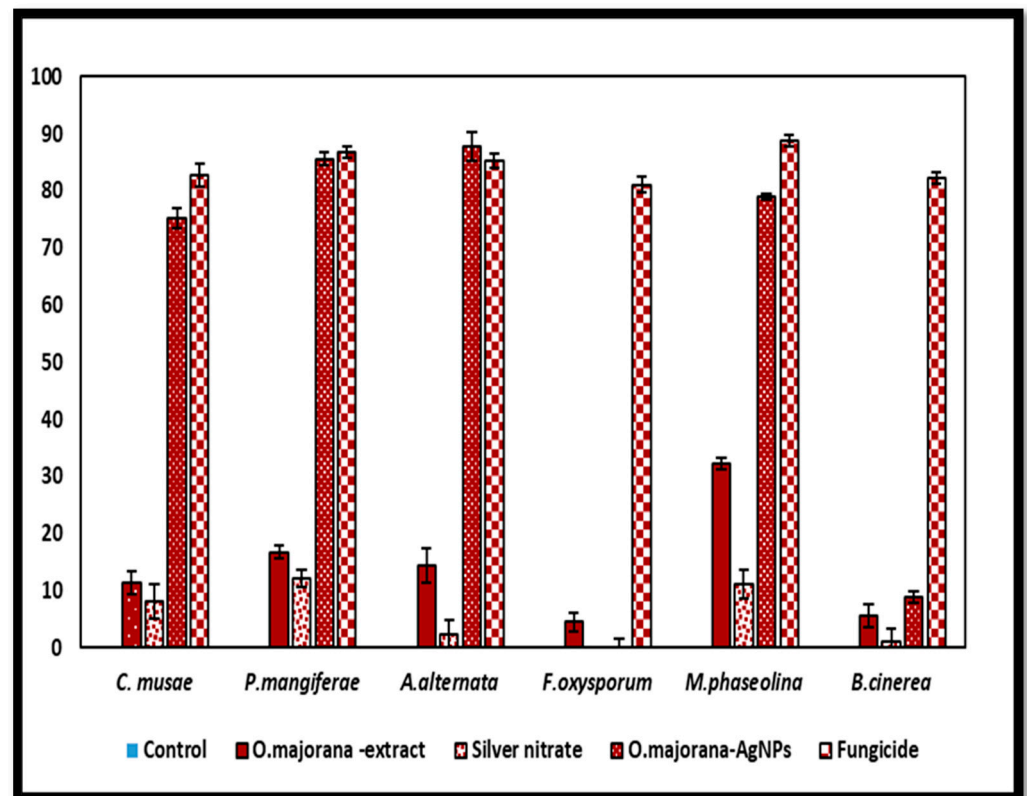


**Figure 9.** Effect of synthesized silver nanoparticles, extract, silver nitrate, and carbendazim-1% on the percent growth inhibition of fungal test isolates. The values are means of three experimental replicates ( $\pm$ SD).

### 3.6. Minimum Inhibitory Concentration (MIC) and Minimum Fungicidal Concentrations (MFC)

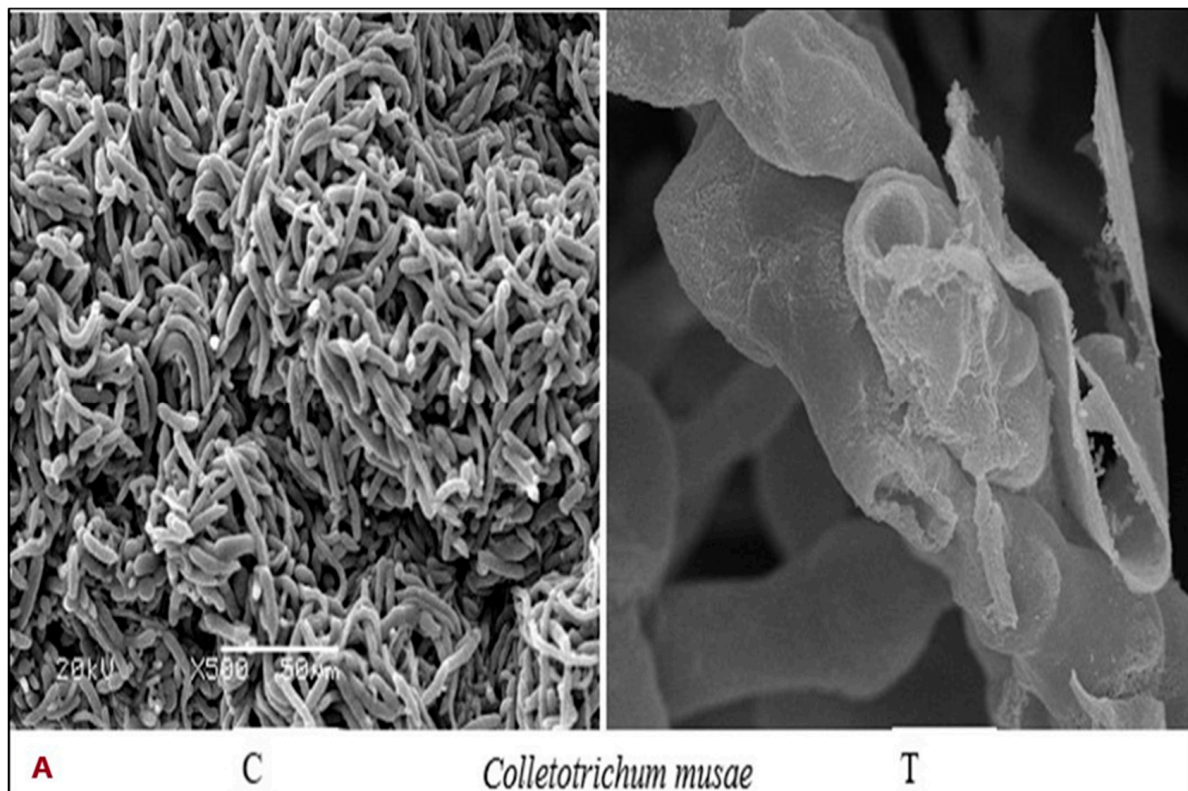
Table 1 shows the minimum inhibitory and minimum fungicidal concentrations of *O. majorana*-AgNPs against several isolates fungal plant pathogens. The MIC of the synthesized AgNPs was determined using a broth dilution assay (Clinical and Laboratory Standards Institute) (CLSI) M38-A2 guidelines [38]. The MIC concentrations for all the test isolates ranged between 2 and 32  $\mu$ g/mL. *Alternaria alternata* and *Pestalotiopsis mangiferae* were inhibited at 2  $\mu$ g/mL. The MIC for *B. cinerea* was the highest at 32  $\mu$ g/mL, while *Fusarium oxysporum* was not inhibited at the highest concentration of 128  $\mu$ g/mL. Correspondingly, the MFC for all the fungal isolates ranged from 4 to 64  $\mu$ g/mL. Similarly, an MIC in the range of 0.25–32  $\mu$ g/mL was reported by AgNPs synthesized from *Cichorium intybus* against *Trichophyton interdigitale*, *T. rubrum*, and *Epidermophyton floccosum* [68]. Essential oil of *O. majorana* inhibited the growth of *Stagonosporopsis cucurbitacearum* and *A. alternata* at 1 mg/mL in a significant manner [69]. The MIC of ethanol leaf extracts of *Prosopis juliflora* against *A. alternata*, *B. cinerea*, *F. oxysporum*, *Aspergillus niger*, *Colletotrichum gloeosporioides*, *Cladosporium cladosporioides*, and *Geotrichum candidum* was recorded between 1–>50 mg/mL. While *A. alternaria* and *B. cinerea* showed the lowest MIC of 0.125 and 1 mg/mL, respectively [70]. The strong antifungal activity demonstrated in the present study authenticates that NPs derived from leaves of *O. majorana* leaves served as potent antifungals against a myriad of fungal isolates. The multitude of phytochemicals could have possibly aided in the synthesis of stable NPs. In accordance with our research, we presume this to be the first report on the antifungal activity of silver nanoparticles on phytopathogenic fungi.

**Table 1.** The MIC and MFC concentrations ( $\mu\text{g/mL}$ ) of synthesized silver NPs against fungal test isolates.

Fungal Isolates	Minimum Inhibitory Concentration (MIC)	Minimum Fungicidal Concentration (MFC)	Minimum Fungicidal Concentration
	<i>O. majorana</i> -AgNPs		Fungicide (Carbendazim)
<i>Colletotrichum musae</i>	$4 \pm 0.00$	$8 \pm 0.00$	$4 \pm 0.00$
<i>Pestalotiopsis mangiferae</i>	$2 \pm 1.15$	$4 \pm 0.00$	$2 \pm 1.15$
<i>Alternaria alternata</i> . f sp. <i>lycopersici</i>	$2 \pm 0.00$	$8 \pm 4.61$	$8 \pm 0.00$
<i>Fusarium oxysporum</i>	NI	NT	$16 \pm 1.15$
<i>Macrophomina phaseolina</i>	$16 \pm 0.00$	$32 \pm 0.00$	$8 \pm 0.00$
<i>Botrytis cinerea</i>	$32 \pm 0.00$	$64 \pm 0.00$	$32 \pm 0.00$

### 3.7. Scanning Electron Microscopy

The effect of synthesized silver nanoparticles on the morphology of the hyphae and spores at their MIC concentration (the concentration before the MBC) was examined with a scanning electron microscope. The microphotographs of control fungal samples (not treated) showed smooth, tubular, and intact hyphae, and the conidia had regular smooth margins without any deformation. However, the micrographs of the treated fungal samples showed that the NPs caused severe damage to the morphology of all the fungal species tested but at different concentrations. *Colletotrichum musae* and *Pestalotiopsis mangiferae* showed heavily peeled and distorted conidia without any contour, while the hyphae were stout, corrugated, and had several bulges (Figure 10A,B). Similarly, totally distorted mycelium with blebs and severe exfoliated conidia with protrusions were seen in the microphotograph of *A. alternata* (Figure 10C). Figure 10D clearly shows deformed, broken hyphae of *M. phaseolina* with very few underdeveloped conidia. The microphotograph of *B. cinerea* shows completely disfigured, leaked, and aggregated conidia and mycelium (Figure 10E).

**Figure 10.** Cont.

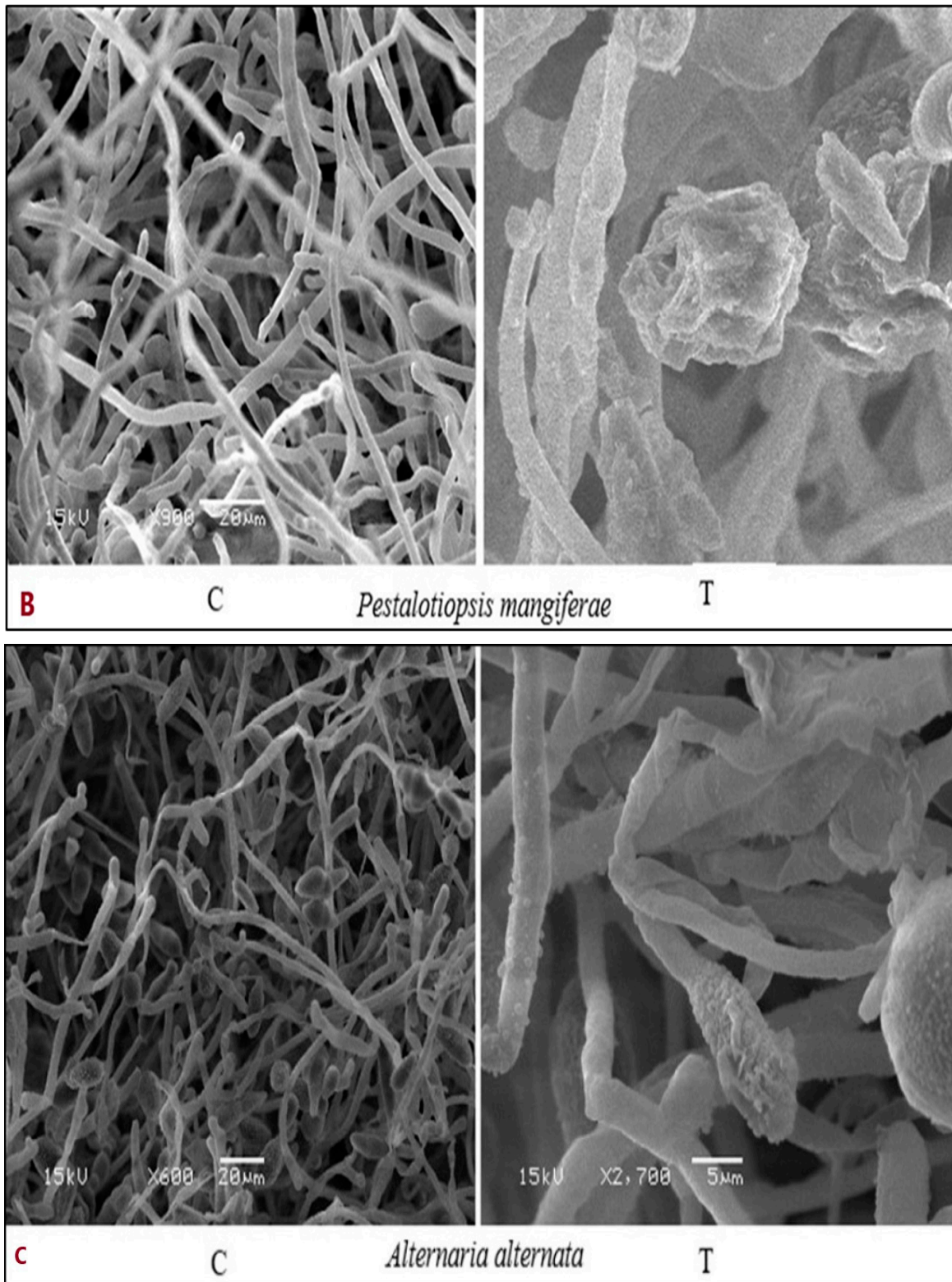
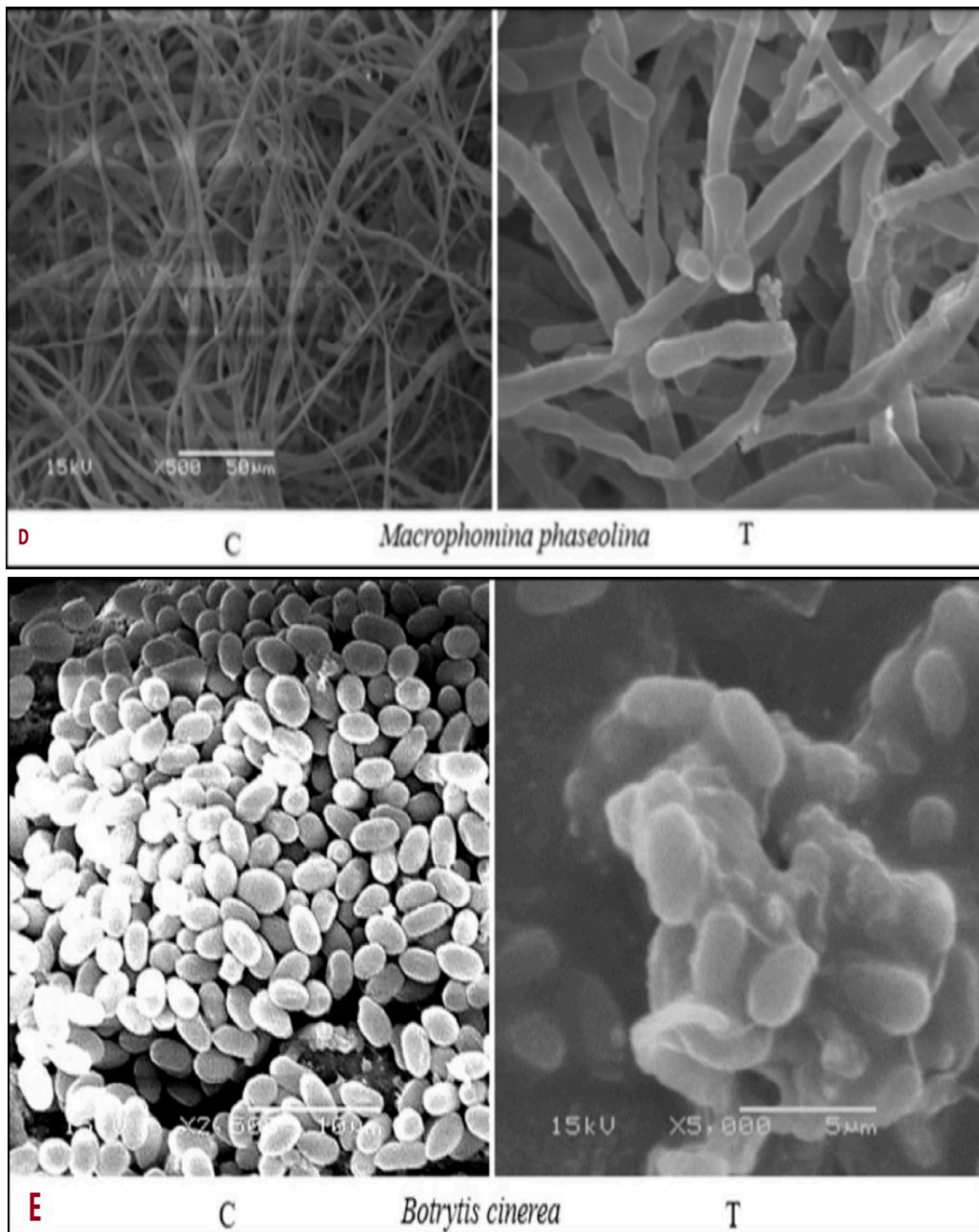


Figure 10. Cont.



**Figure 10.** Scanning electron microphotographs of different fungal isolates treated with biosynthesized AgNPs. Severe morphological alterations in the structure of mycelium and conidia were witnessed. Images: (A) *Colletotrichum musae*, (B) *Pestalotiopsis mangiferae*, (C) *Alternaria alternata*, (D) *Macrophomina phaseolina*, (E) *Botrytis cinerea*. C—control (not treated), T—treated with *O. majorana*-AgNPs.

Similar to the present study, morphological alternations in hyphae and conidia were witnessed in fungal isolates treated with plant extracts and nanoparticles [22,71,72]. Silver nanoparticles (AgNPs) prepared using orange and pomegranate showed strong fungicidal effects on *Alternaria solani* at 100  $\mu\text{g}/\text{mL}$ . The treated *A. solani* showed distorted, plasmolyzed, collapsed, and dead fungal hyphae [22]. In another study, biogenic sil-

ver nanoparticles caused destructive effects on the mycelium and conidia of *Aspergillus flavus* [73]. Copper nanoparticles showed prominent changes in the fungal morphology of *Neofusicoccum* sp., *Fusarium solani* and *F. oxysporum*, the treated hyphae showed shrunken hyphae with bulges, cellular leakage, and deformed mycelium and conidia [71]. Previous studies have also shown degeneration of fungal filaments of *A. fumigatus*, *Candidia albicans*, *Trichophyton rubrum*, and *T. mentagrophytes* when treated with components of *Scutellaria baicalensis* Georgi root [74].

The prominent fungal morphological destruction caused by *O. majorana*-AgNPs in the current study could be attributed to the nano size of the synthesized AgNPs and the adherence property of the silver ions released from AgNPs. Several modes of action have been proposed to explain the antifungal mechanisms of AgNPs. The stability and osmotic balance of a fungal cell primarily depend on the cell wall and cell membrane. It was stated that when the AgNPs come into contact with the fungal cell surface, silver ions are released, which then connect to cell surfaces through adhesions. These adhesions disturb the cell wall components, primarily the chitin, resulting in osmotic imbalance and disfigured and malformed fungal cells [75]. Secondly, the NPs themselves can destroy the cell membrane, enter the cell, and interact with different cellular components of the cell, including DNA, RNA, proteins, and lipids, causing cell leakage and death [76,77]. *Fusarium graminearum* treated with AgNPs incited the expression of reactive oxygen species generation and azole-related ATP-binding cassette (ABC) transporters, resulting in compromised development of cell structures and metabolic pathways [78]. The morphological changes induced in microorganisms after AgNP interaction are often characterized by plasmolysis (cytoplasm shrinkage), membrane detachment and cell wall rupture [79]. The efficacy of *O. majorana*-AgNPs in targeting the phytopathogenic fungi collectively could be because of their shape, nanosize, and the phytochemicals present in *O. majorana* extracts, which served as excellent coating agents.

#### 4. Conclusions

Nanotechnology innovations have opened the door for the utilization and application of nanoparticles in the agricultural sector. The development of nanofungicides and their use in the control of phytopathogenic fungi is a targeted, low-toxicity approach. The robust antifungal activity displayed by synthesized AgNPs against several plant pathogens in this study suggests their potential to be developed as nanofungicides to control plant damage caused by fungi. Furthermore, the process of synthesis was very quick, and the abundant biomolecules present in *O. majorana* could have assisted in reducing and capping during nanosynthesis. Based on the antifungal findings and scanning electron microscopy studies, synthesized AgNPs have the potential to be formulated as safe, cost-effective herbal nanofungicides against resistant strains of phytopathogenic fungi in the management of plant diseases. However, more research into their mode of action and safety evaluation is required in the future.

**Author Contributions:** Conceptualization and design, H.R.; Data curation, H.A.A. and N.S.A.; Formal analysis, T.A. and H.A.A.; Funding acquisition, M.S.A.; Investigation, R.R., T.A., N.S.A., H.A.A. and R.R.; Methodology, R.M.A., H.R., T.A. and M.S.A.; Project administration, M.S.A. and H.R.; Resources, T.A., H.A.A., N.S.A. and R.M.A.; Software, T.A., R.R. and N.S.A.; Supervision, H.R. and M.S.A.; Validation, R.M.A. and H.R.; Visualization, R.M.A. and R.R.; Writing and preparing—original draft, H.R.; Writing—review and editing, R.M.A. and M.S.A. All authors have read and agreed to the published version of the manuscript.

**Funding:** This research project was funded by the Researchers Support Project (number RSP 2021/173) of King Saud University, Riyadh, Saudi Arabia, for payment of the charge for publishing this manuscript.

**Institutional Review Board Statement:** Not applicable.

**Informed Consent Statement:** Not applicable.

**Data Availability Statement:** All the data of the present study are present in the manuscript.

**Acknowledgments:** The authors extend their appreciation to the Researchers Support Project number RSP 2021/173) of King Saud University for funding this research.

**Conflicts of Interest:** The authors declare no conflict of interest.

**Sample Availability:** Samples of the compounds are available from the author.

## References

1. Chouhan, D.; Dutta, A.; Kumar, A.; Mandal, P.; Choudhuri, C. Application of nickel chitosan nanoconjugate as an antifungal agent for combating *Fusarium* rot of wheat. *Sci. Rep.* **2022**, *12*, 14518. [[CrossRef](#)] [[PubMed](#)]
2. Muhammad, A.; Isra, N.; Shahbaz, T.S.; Nasir, A.R.; Ehsan, H.; Muhammad, U.; Hamza, S.; Kiran, F.; Ehtsham, A.; Abdul, Q. Nanoparticles: A safe way towards fungal diseases. *Arch. Phytopathol. Plant Prot.* **2020**, *53*, 781–792.
3. Al Otibi, F.; Rizwana, H.; Alharbi, R.I.; Alshaiikh, N.; Albasher, G. Antifungal Effect of *Saussurea lappa* Roots Against Phytopathogenic Fungi and Resulting Morphological and Ultrastructural Changes. *Gesunde Pflanzen.* **2020**, *72*, 57–67. [[CrossRef](#)]
4. Li, J.; Gu, F.; Wu, R.; Yang, J.; Zhang, K. Phylogenomic evolutionary surveys of subtilase superfamily genes in fungi. *Sci. Rep.* **2017**, *7*, 45456. [[CrossRef](#)]
5. Zubrod, J.P.; Bundschuh, M.; Arts, G.; Brühl, C.A.; Imfeld, G.; Knäbel, A.; Payraudeau, S.; Rasmussen, J.J.; Rohr, J.; Scharmüller, A.; et al. Fungicides: An Overlooked Pesticide Class? *Environ. Sci. Technol.* **2019**, *53*, 3347–3365. [[CrossRef](#)]
6. Anand, G.; Rajeshkumar, K.C. Challenges and Threats Posed by Plant Pathogenic Fungi on Agricultural Productivity and Economy. In *Fungal Diversity, Ecology and Control Management*; Springer: Singapore, 2022; Volume 1, pp. 483–493.
7. Shang, Y.; Kamrul Hasan, M.; Ahammed, G.J.; Li, M.; Yin, H.; Zhou, J. Applications of nanotechnology in plant growth and crop protection: A review. *Molecules* **2019**, *24*, 2558. [[CrossRef](#)]
8. Ahmed, H.M.; Roy, A.; Wahab, M.; Ahmed, M.; Qadir, G.O.; Elesawy, B.H.; Uddin Khandaker, M.; Islam, M.N.; Emran, T.B. Applications of Nanomaterials in Agrifood and Pharmaceutical Industry. *J. Nanomater.* **2021**, *2021*, 1472096. [[CrossRef](#)]
9. Alghuthaymi, M.A.; Kalia, A.; Bhardwaj, K.; Bhardwaj, P.; Abd-Elsalam, K.A.; Valis, M.; Kuca, K. Nanohybrid antifungals for control of plant diseases: Current status and future perspectives. *J. Fungi* **2021**, *7*, 48. [[CrossRef](#)]
10. Worrall, E.A.; Hamid, A.; Mody, K.T.; Mitter, N.; Pappu, H.R. Nanotechnology for plant disease management. *Agronomy* **2018**, *8*, 285. [[CrossRef](#)]
11. Pestovsky, Y.S.; Martínez-Antonio, A. The Use of Nanoparticles and Nanoformulations in Agriculture. *J. Nanosci. Nanotechnol.* **2017**, *17*, 8699–8730. [[CrossRef](#)]
12. Wang, X.; Liu, J.; Chen, H.; Han, H.; Yuan, Z. Evaluation and mechanism of antifungal effects of carbon nanomaterials in controlling plant fungal pathogen. *Carbon* **2014**, *68*, 798–806. [[CrossRef](#)]
13. Bryaskova, R.; Pencheva, D.; Nikolov, S.; Kantardjiev, T. Synthesis and comparative study on the antimicrobial activity of hybrid materials based on silver nanoparticles (AgNps) stabilized by polyvinylpyrrolidone (PVP). *J. Chem. Biol.* **2011**, *4*, 185–191. [[CrossRef](#)] [[PubMed](#)]
14. Hao, Y.; Cao, X.; Ma, C.; Zhang, Z.; Zhao, N.; Ali, A.; Hou, T.; Xiang, Z.; Zhuang, J.; Wu, S.; et al. Potential Applications and Antifungal Activities of Engineered Nanomaterials against Gray Mold Disease Agent *Botrytis cinerea* on Rose Petals. *Front. Plant Sci.* **2017**, *8*, 1332. [[CrossRef](#)] [[PubMed](#)]
15. Jo, Y.; Kim, B.H.; Jung, G. Antifungal activity of silver ions and nanoparticles on phytopathogenic fungi. *Plant Dis.* **2009**, *93*, 1037–1043. [[CrossRef](#)] [[PubMed](#)]
16. Guilger-Casagrande, M.; Lima, R.D. Synthesis of silver nanoparticles mediated by fungi: A review. *Front. Bioeng. Biotechnol.* **2019**, *7*, 287. [[CrossRef](#)] [[PubMed](#)]
17. Ahmed, S.; Ahmad, M.; Swami, B.L.; Ikram, S. A review on plants extract mediated synthesis of silver nanoparticles for antimicrobial applications: A green expertise. *J. Adv. Res.* **2016**, *7*, 17–28. [[CrossRef](#)] [[PubMed](#)]
18. Siddiqi, K.S.; Rahman, A.; Tajuddin Husen, A. Biogenic fabrication of iron/iron oxide nanoparticles and their application. *Nanoscale Res. Lett.* **2016**, *11*, 498. [[CrossRef](#)] [[PubMed](#)]
19. Mishra, S.; Keswani, C.; Abhilash, P.C.; Fraceto, L.F.; Singh, H.B. Integrated approach of agri-nanotechnology: Challenges and future trends. *Front. Plant Sci.* **2017**, *8*, 471. [[CrossRef](#)]
20. El Shafey, A.M. Green synthesis of metal and metal oxide nanoparticles from plant leaf extracts and their applications: A review. *Green Process. Synth.* **2020**, *9*, 304–339. [[CrossRef](#)]
21. Kaur, P.M.K.; Sidhu, A.K. Green synthesis: An eco-friendly route for the synthesis of iron oxide nanoparticles. *Front. Nanotechnol.* **2021**, *3*, 655062.
22. Mostafa, Y.S.; Alamri, S.A.; Alrumman, S.A.; Hashem, M.; Baka, Z.A. Green Synthesis of Silver Nanoparticles Using Pomegranate and Orange Peel Extracts and Their Antifungal Activity against *Alternaria solani*, the Causal Agent of Early Blight Disease of Tomato. *Plants* **2021**, *10*, 2363. [[CrossRef](#)] [[PubMed](#)]
23. Nguyen, D.H.; Lee, J.S.; Park, K.D.; Ching, Y.C.; Nguyen, X.T.; Phan, V.; Hoang Thi, T.T. Green Silver Nanoparticles Formed by *Phyllanthus urinaria*, *Pouzolzia zeylanica*, and *Scoparia dulcis* Leaf Extracts and the Antifungal Activity. *Nanomaterials* **2020**, *10*, 542. [[CrossRef](#)] [[PubMed](#)]

24. Renganathan, S.; Subramaniyan, S.; Karunanithi, N.; Vasanthakumar, P.; Kutzner, A.; Kim, P.S.; Heese, K. Antibacterial, Antifungal, and Antioxidant Activities of Silver Nanoparticles Biosynthesized from *Bauhinia tomentosa* Linn. *Antioxidants* **2021**, *10*, 1959. [[CrossRef](#)] [[PubMed](#)]
25. Wang, L.; Lu, F.; Liu, Y.; Wu, Y.; Wu, Z. Photocatalytic degradation of organic dyes and antimicrobial activity of silver nanoparticles fast synthesized by flavonoids fraction of *Psidium guajava* L. leaves. *J. Mol. Liq.* **2018**, *263*, 187–192. [[CrossRef](#)]
26. Cala Peralta, A.; Salcedo, J.R.; Torres Martínez, A.; Varela Montoya, R.M.; González Molinillo, J.M.; Macías Domínguez, F.A. A study on the phytotoxic potential of the seasoning herb marjoram (*Origanum majorana* L.) leaves. *Molecules* **2021**, *26*, 3356. [[CrossRef](#)]
27. Algebaly, A.; Algabbani, Q.; Al-Otaibi, W.R.; Alotaibi, A.M.; Albani, F.G.; ALanazi, I.S.; Al-Qahtani, W.S. Aqueous Extract of *Origanum majorana* at Low Temperature (0 °C) Promotes Mitochondrial Fusion and Contributes to Induced Apoptosis in Human Breast Cancer Cells. *Asian. Pac. J. Cancer. Prev.* **2021**, *22*, 2959. [[CrossRef](#)]
28. Haj-Husein, I.; Tukan, S.; Alkazaleh, F. The effect of marjoram (*Origanum majorana*) tea on the hormonal profile of women with polycystic ovary syndrome: A randomized controlled pilot study. *J. Hum. Nutr. Diet.* **2016**, *29*, 105–111. [[CrossRef](#)]
29. Della Pepa, T.; Elshafie, H.S.; Capasso, R.; De Feo, V.; Camele, I.; Nazzaro, F.; Scognamiglio, M.R.; Caputo, L. Antimicrobial and Phytotoxic Activity of *Origanum heracleoticum* and *O. majorana* Essential Oils Growing in Cilento (Southern Italy). *Molecules* **2019**, *24*, 2576. [[CrossRef](#)]
30. Vági, E.; Simándi, B.; Suhajda, A.; Hethelyi, E. Essential oil composition and antimicrobial activity of *Origanum majorana* L. extracts obtained with ethyl alcohol and supercritical carbon dioxide. *Food. Res. Int.* **2005**, *38*, 51–57. [[CrossRef](#)]
31. Leeja, L.; Thoppil, J.E. Antimicrobial activity of methanol extract of *Origanum majorana* L. (Sweet marjoram). *J. Environ. Biol.* **2007**, *28*, 145.
32. Richter, J.; Schellenberg, I. Comparison of different extraction methods for the determination of essential oils and related compounds from aromatic plants and optimization of solid-phase microextraction/gas chromatography. *Anal. Bioanal. Chem.* **2007**, *387*, 2207–2217. [[CrossRef](#)] [[PubMed](#)]
33. Assaf, M.H.; Ali, A.A.; Makboul, M.A.; Beck, J.P.; Anton, R. Preliminary study of phenolic glycosides from *Origanum majorana*, quantitative estimation of arbutin; cytotoxic activity of hydroquinone. *Planta. Med.* **1987**, *53*, 343–345. [[CrossRef](#)] [[PubMed](#)]
34. Hajlaoui, H.; Mighri, H.; Aouni, M.; Gharsallah, N.; Kadri, A. Chemical composition and in vitro evaluation of antioxidant, antimicrobial, cytotoxicity and anti-acetylcholinesterase properties of Tunisian *Origanum majorana* L. essential oil. *Microb. Pathog.* **2016**, *95*, 86–94. [[CrossRef](#)] [[PubMed](#)]
35. Bouyahya, A.; Chamkhi, I.; Benali, T.; Guaouguaou, F.E.; Balahbib, A.; El Omari, N.; Taha, D.; Belmehdi, O.; Ghokhan, Z.; al El Menyiy, N. Traditional use, phytochemistry, toxicology, and pharmacology of *Origanum majorana* L. *J. Ethnopharmacol.* **2021**, *265*, 113318. [[CrossRef](#)]
36. Van-Son, J.; Nyklíček, I.; Pop, V.J.; Pouwer, F. Testing the effectiveness of a mindfulness-based intervention to reduce emotional distress in outpatients with diabetes (DiaMind): Design of a randomized controlled trial. *BMC Public Health* **2011**, *11*, 131. [[CrossRef](#)]
37. Kim, S.W.; Jung, J.H.; Lamsal, K.; Kim, Y.S.; Min, J.S.; Lee, Y.S. Antifungal effects of silver nanoparticles (AgNPs) against various plant pathogenic fungi. *Mycobiology* **2012**, *40*, 53–58. [[CrossRef](#)]
38. Clinical and Laboratory Standards Institute (CLSI). *Reference Method for Broth Dilution Antifungal Susceptibility Testing of Filamentous Fungi*, 3rd ed.; Document M38-A2; Clinical and Laboratory Standards Institute: Wayne, PA, USA, 2017.
39. Espinel-Ingroff, A.; Fothergill, A.; Peter, J.; Rinaldi, M.G.; Walsh, T.J. Testing conditions for determination of minimum fungicidal concentrations of new and established antifungal agents for *Aspergillus* spp.: NCCLS collaborative study. *J. Clin. Microbiol.* **2002**, *40*, 3204–3208. [[CrossRef](#)]
40. Zahran, M.; El-Kemary, M.; Khalifa, S.; El-Seedi, H. Spectral studies of silver nanoparticles biosynthesized by *Origanum majorana*. *Green. Process. Synth.* **2018**, *7*, 100–105. [[CrossRef](#)]
41. Sooraj, M.P.; Nair, A.S.; Vineetha, D.J.C.P. Sunlight-mediated green synthesis of silver nanoparticles using *Sida retusa* leaf extract and assessment of its antimicrobial and catalytic activities. *Chem. Pap.* **2021**, *75*, 351–363. [[CrossRef](#)]
42. El-Seedi, H.R.; El-Shabasy, R.M.; Khalifa, S.A.; Saeed, A.; Shah, A.; Shah, R.; Iftikhar, F.J.; Ab-del-Daim, M.M.; Omri, A.; Hajrahand, N.H.; et al. Metal nanoparticles fabricated by green chemistry using natural extracts: Biosynthesis, mechanisms, and applications. *RSC. Adv.* **2019**, *9*, 24539–24559. [[CrossRef](#)]
43. Bahuguna, G.; Kumar, A.; Mishra, N.K.; Kumar, C.; Bahlwal, A.; Chaudhary, P.; Singh, R. Green synthesis and characterization of silver nanoparticles using aqueous petal extract of the medicinal plant *Combretum indicum*. *Mater. Res. Express* **2016**, *3*, 075003. [[CrossRef](#)]
44. Prathna, T.C.; Raichur, A.M.; Chandrasekaran, N.; Mukherjee, A. Sunlight Irradiation Induced Green Synthesis of Stable Silver Nanoparticles Using *Citrus limon*. Extract. *Proc. Natl. Acad. Sci. India Sect. B Biol. Sci.* **2014**, *84*, 65–70. [[CrossRef](#)]
45. Karimi Zarchi, A.A.; Mokhtari, N.; Arfan, M.; Rehman, T.U.; Ali, M.; Amini, M.; Faridi Majidi, R.; Shahverdi, A.R. A sunlight-induced method for rapid biosynthesis of silver nanoparticles using an *Andrachnea chordifolia* ethanol extract. *Appl. Phys. A* **2011**, *103*, 349–353. [[CrossRef](#)]
46. Dong, S.; Tang, C.; Zhou, H.; Zhao, H. Photochemical synthesis of gold nanoparticles by the sunlight radiation using a seeding approach. *Gold. Bull.* **2004**, *37*, 187–195. [[CrossRef](#)]

47. Alharbi, N.S.; Alsubhi, N.S.; Felimban, A.I. Green synthesis of silver nanoparticles using medicinal plants: Characterization and application. *J. Radiat. Res. Appl. Sci.* **2022**, *15*, 109–124. [[CrossRef](#)]
48. Lade, B.D.; Shanware, A.S. Phytonanofabrication: Methodology and Factors Affecting Biosynthesis of Nanoparticles. In *Smart Nanosystems for Biomedicine, Optoelectronics and Catalysis*; Shabatina, T., Bochenkov, V., Eds.; IntechOpen: London, UK, 2020. [[CrossRef](#)]
49. Oves, M.; Rauf, M.A.; Aslam, M.; Qari, H.A.; Sonbol, H.; Ahmad, I.; Zaman, G.S.; Saeed, M. Green synthesis of silver nanoparticles by *Conocarpus lancifolius* plant extract and their antimicrobial and anti-cancer activities. *Saudi J. Biol. Sci.* **2022**, *29*, 460–471. [[CrossRef](#)]
50. Vasylyev, G.S.; Vorobyova, V.I.; Skiba, M.I.; Khrokalo, L. Green synthesis of silver nanoparticles using waste products (Apricot and Black Currant Pomace) aqueous extracts and their characterization. *Adv. Mater. Sci. Eng.* **2020**, *3*, 1–11. [[CrossRef](#)]
51. Rizwana, H.; Bokahri, N.A.; Alkhattaf, F.S.; Albasher, G.; Aldehaish, H.A. Antifungal, Antibacterial, and Cytotoxic Activities of Silver Nanoparticles Synthesized from Aqueous Extracts of Mace-Arils of *Myristica fragrans*. *Molecules* **2021**, *26*, 7709. [[CrossRef](#)]
52. Singh, D.; Rawat, D. Microwave-assisted synthesis of silver nanoparticles from *Origanum majorana* and *Citrus sinensis* leaf and their antibacterial activity: A green chemistry approach. *Bioresour. Bioprocess.* **2016**, *3*, 14. [[CrossRef](#)]
53. Yassin, M.T.; Mostafa, A.A.F.; Al-Askar, A.A.; Al-Otibi, F.O. Facile green synthesis of silver nanoparticles using aqueous leaf extract of *Origanum majorana* with potential bioactivity against multidrug resistant bacterial strains. *Crystals* **2022**, *12*, 603. [[CrossRef](#)]
54. Aseyd Nezhad, S.; Es-haghi, A.; Tabrizi, M.H. Green synthesis of cerium oxide nanoparticle using *Origanum majorana* L. leaf extract, its characterization and biological activities. *Appl. Organometal. Chem.* **2019**, *34*, e5314.
55. Jemilugba, O.T.; Parani, S.; Mavumengwana, V.; Oluwafemi, O.S. Green synthesis of silver nanoparticles using *Combretum erythrophyllum* leaves and its antibacterial activities. *Colloid Interface Sci. Commun.* **2019**, *31*, 100191. [[CrossRef](#)]
56. Liu, W.B.; Rose, J.; Plantevin, S.; Auffan, M.; Bottero, J.Y.; Vidaud, C. Protein corona formation for nanomaterials and proteins of a similar size: Hard or soft corona? *Nanoscale* **2013**, *5*, 1658–1668. [[CrossRef](#)] [[PubMed](#)]
57. Dalstein, L.; Ben Haddada, M.; Barbillon, G.; Humbert, C.; Tadjeddine, A.; Boujday, S.; Busson, B. Revealing the interplay between adsorbed molecular layers and gold nanoparticles by linear and nonlinear optical properties. *J. Phys. Chem.* **2015**, *119*, 17146–17155. [[CrossRef](#)]
58. Shah, M.; Nawaz, S.; Jan, H.; Uddin, N.; Ali, A.; Anjum, S.; Giglioli-Guivarc'h, N.; Hano, C.; Abbasi, B.H. Synthesis of bio-mediated silver nanoparticles from *Silybum marianum* and their biological and clinical activities. *Mater. Sci. Eng. C* **2020**, *112*, 1108899. [[CrossRef](#)]
59. Erenler, R.; Dag, B. Biosynthesis of silver nanoparticles using *Origanum majorana* L. and evaluation of their antioxidant activity. *Inorg. Nano-Met. Chem.* **2022**, *52*, 485–492.
60. Deljou, A.; Goudarzi, S. Green Extracellular Synthesis of the Silver Nanoparticles Using Thermophilic *Bacillus* sp. AZ1 and its Antimicrobial Activity Against Several Human Pathogenetic Bacteria. *Iran. J. Biotechnol.* **2016**, *14*, 25–32. [[CrossRef](#)]
61. Rizwana, H.; Alwhibi, M.S.; Aldarson, H.A.; Awad, M.A.; Soliman, D.A.; Bhat, R.S. Green synthesis, characterization, and antimicrobial activity of silver nanoparticles prepared using *Trigonella foenum-graecum* L. leaves grown in Saudi Arabia. *Green. Process. Synth.* **2021**, *10*, 421–429. [[CrossRef](#)]
62. Rizwana, H.; Bokahri, N.A.; Alfarhan, A.; Aldehaish, H.A.; Alsaggabi, N.S. Biosynthesis and characterization of silver nanoparticles prepared using seeds of *Sisymbrium irio* and evaluation of their antifungal and cytotoxic activities. *Green. Process. Synth.* **2022**, *11*, 478–491. [[CrossRef](#)]
63. Femi-Adepoju, A.G.; Dada, A.O.; Otun, K.O.; Adepoju, A.O.; Fatoba, O.P. Green synthesis of silver nanoparticles using terrestrial fern (*Gleichenia Pectinata* (Willd.) C. Presl.): Characterization and antimicrobial studies. *Heliyon* **2019**, *5*, e01543. [[CrossRef](#)]
64. El-Ghorab, A.H.; Behery, F.A.; Abalgawad, M.A.; Alsohaimi, I.H.; Musa, A.; Mostafa, E.M.; Aboseada, M.A. LV/MS Profiling and Gold Nanoparticles Formation of Major Metabolites from *Origanum majorana* as Antibacterial and Antioxidant Potentialities. *Plants* **2022**, *11*, 1871. [[CrossRef](#)] [[PubMed](#)]
65. Kaskatepe, B.; Aslan Erdem, S.; Ozturk, S.; Safi Oz, Z.; Subasi, E.; Koyuncu, M.; Vlainić, J.; Kosalec, I. Antifungal and Anti-Virulent Activity of *Origanum majorana* L. Essential Oil on *Candida albicans* and In Vivo Toxicity in the *Galleria mellonella* Larval Model. *Molecules* **2022**, *27*, 663. [[CrossRef](#)] [[PubMed](#)]
66. Taha, A.S.; Abo-Elgat, W.A.A.; Fares, Y.G.D.; Saleem, M.Z.M. Isolated essential oils as antifungal compounds for organic materials. *Biomass Conv. Bioref.* **2022**. [[CrossRef](#)]
67. Rizwana, H.; Alwhibi, M.S. Biosynthesis of silver nanoparticles using leaves of *Mentha pulegium*, their characterization, and antifungal properties. *Green. Process. Synth.* **2021**, *10*, 824–834. [[CrossRef](#)]
68. Mahmoudi, S.; Vahidi, M.; Malekabad, E.S.; Izadi, A.; Khatami, M.; Dadashi, A. In Vitro Antifungal Activity of Green Synthesized Silver Nanoparticles in Comparison to Conventional Antifungal Drugs Against *Trichophyton interdigitale*, *Trichophyton rubrum* and *Epidermophyton floccosum*. *Infect. Disord. Drug Targets* **2021**, *21*, 370–374. [[CrossRef](#)]
69. Moumni, M.; Romanazzi, G.; Najar, B.; Pistelli, L.; Ben Amara, H.; Mezrioui, K.; Karous, O.; Chaieb, I.; Allagui, M.B. Antifungal Activity and Chemical Composition of Seven Essential Oils to Control the Main Seedborne Fungi of Cucurbits. *Antibiotics* **2021**, *10*, 104. [[CrossRef](#)] [[PubMed](#)]
70. Saleh, I.; Abu-Dieyeh, M.H. Novel *Prosopis juliflora* leaf ethanolic extract as natural antimicrobial agent against food spoiling microorganisms. *Sci. Rep.* **2021**, *11*, 7871. [[CrossRef](#)]

71. Pariona, N.; Mtz-Enriquez, A.I.; Sánchez-Rangelac, D.; Carrión, G.; Paraguay-Delgado, F.; Rosas-Saitoa, G. Green-synthesized copper nanoparticles as a potential antifungal against plant pathogens. *RSC Adv.* **2019**, *9*, 18835–18843. [[CrossRef](#)]
72. Alotibi, F.; Rizwana, H. Chemical Composition, FTIR Studies, Morphological Alterations, and Antifungal Activity of Leaf Extracts of *Artemisia sieberi* from Saudi Arabia. *Int. J. Agric. Biol.* **2019**, *21*, 1241–1248.
73. Al-Othman, M.R.; Abd El-Aziz, A.R.M.; Mahmoud, M.A.; Eifan, S.A.; El-Shikh, M.S.; Majrashi, M. Application of silver nanoparticles as antifungal and antiaflatoxin B1 produced by *Aspergillus flavus*. *Dig. J. Nanomater Bios.* **2014**, *9*, 151–157.
74. Da, X.; Nishiyama, Y.; Tie, D.; Hein, K.Z.; Yamamoto, O.; Morita, E. Antifungal activity and mechanism of action of Ou-gon (*Scutellaria* root extract) components against pathogenic fungi. *Sci. Rep.* **2019**, *9*, 1683. [[CrossRef](#)] [[PubMed](#)]
75. Bowman, S.M.; Free, S.J. The structure and synthesis of the fungal cell wall. *Bioessays.* **2006**, *28*, 799–808. [[CrossRef](#)] [[PubMed](#)]
76. Patra, P.; Mitra, S.; Debnath, N.; Goswami, A. Biochemical-, biophysical-, and microarray-based anti-fungal evaluation of the buffer-mediated synthesized nano zinc oxide: An in vivo and in vitro toxicity study. *Langmuir* **2012**, *28*, 16966–16978. [[CrossRef](#)] [[PubMed](#)]
77. Bhabra, G.; Sood, A.; Fisher, B.; Cartwright, L.; Saunders, M.; Evans, W.H.; Case, C.P. Nanoparticles can cause DNA damage across a cellular barrier. *Nat. Nanotechnol.* **2009**, *4*, 876–883. [[CrossRef](#)]
78. Jiang, Y.; Zhou, P.; Zhang, P.; Adeel, M.; Shakoor, N.; Li, Y.; Li, M.; Guo, M.; Zhao, W.; Lou, B.; et al. Green synthesis of metal-based nanoparticles for sustainable agriculture. *Environ. Pollut.* **2022**, *309*, 119755. [[CrossRef](#)]
79. Mikhailova, E.O. Silver Nanoparticles: Mechanism of Action and Probable Bio-Application. *J. Funct. Biomater.* **2020**, *11*, 84. [[CrossRef](#)]